



# THE SKELETAL MORPHOLOGY OF THE SOLEMYDID TURTLE *NAOMICHELYS SPECIOSA* FROM THE EARLY CRETACEOUS OF TEXAS

WALTER G. JOYCE,<sup>1</sup> JULIANA STERLI,<sup>2</sup> AND SANDRA D. CHAPMAN<sup>3</sup>

<sup>1</sup>Department of Geosciences, University of Fribourg, Chemin du Musée 6, 1700 Fribourg, Switzerland, <walter.joyce@unifr.ch>; <sup>2</sup>CONICET, Museo Paleontológico Egidio Feruglio, Av. Fontana 140, 9100 Trelew, Chubut Province, Argentina, <jsterli@mef.org.ar>; and <sup>3</sup>Department of Palaeontology, Natural History Museum, London SW7 5BD, UK, <s.chapman@nhm.ac.uk>

**ABSTRACT**— The fossil record of solemydid turtles is primarily based on isolated fragments collected from Late Jurassic to Late Cretaceous sediments throughout North America and Europe and little is therefore known about the morphology and evolutionary history of the group. We here provide a detailed description of the only known near-complete solemydid skeleton, which was collected from the Lower Cretaceous (Aptian–Albian) Antlers Formation of Texas during the mid-twentieth century, but essentially remains undescribed to date. Though comparison is limited, the skeleton is referred to *Naomichelys speciosa*, which is based on an isolated entoplastron from the Lower Cretaceous (Aptian–Albian) Kootenai (Cloverly) Formation of Montana. The absence of temporal emarginations, contribution of the jugals to the orbits, and a clear subdivision of the middle and inner cavities, and the presence of elongate postorbitals, posteriorly expanded squamosals, a triangular fossa at the posterior margin of the squamosals, an additional pair of tubercula basioccipitale that is formed by the pterygoids, foramina pro ramo nervi vidiani (VII) that are visible in ventral view, shell sculpturing consisting of high tubercles, a large entoplastron with entoplastral scute, V-shaped anterior peripherals, and limb osteoderms with tubercular sculpture diagnose *Naomichelys speciosa* as a representative of Solemydidae. The full visibility of the parabasisphenoid complex in ventral view, the presence of an expanded symphyseal shelf, and the unusual ventromedial folding of the coronoid process are the primary characteristics that distinguish *Naomichelys speciosa* from the near-coeval European taxon *Helochelydra nopcsai*.

## INTRODUCTION

**S**OLEMYDIDAE is a group of large-bodied (carapace length ~60–80 cm) Late Jurassic to Late Cretaceous turtles currently best diagnosed by the presence of distinct tubercles that decorate the surface of the cranium, shell, and osteoderms (Joyce et al., 2011). The existence of the group was only recognized recently (Lapparent de Broin and Murelaga, 1996, 1999) and its restricted occurrence in North America and Europe testifies to the faunal connections between those two continents during the Late Mesozoic (Hirayama et al., 2000). The vast majority of known solemydid material consists of fragments (Joyce et al., 2011) and little is therefore known about the skeletal morphology and phylogenetic relationships of the representatives of this group.

An isolated, partial entoplastron (AMNH 6136; Hay, 1908, pl. 40, figs. 2, 3) collected near Pryor, Montana represents the first known solemydid material from North America and also the type of the only named North American taxon, *Naomichelys speciosa* Hay, 1908. The type material was at first reported as originating from the Late Jurassic Morrison Formation, but a recent review demonstrated that the specimen was collected from the Lower Cretaceous (Aptian) Kootenai (or Cloverly) Formation instead (Joyce et al., 2011). Fragmentary solemydid remains have since been reported from numerous Aptian to Cenomanian localities throughout North America and have been referred to *Naomichelys* or *N. speciosa* for a lack of competing taxa (Joyce et al., 2011). The spatial distribution of this material is summarized in Figure 1.

The Lower Cretaceous (Aptian–Albian) Antlers Formation (also known as the Trinity Sand) of Texas and Oklahoma has yielded a moderately rich terrestrial fauna consisting of fish, amphibians, lepidosaurs, turtles, dinosaurs, and mammals (e.g., Gaffney, 1972; Cifelli et al., 1997; Nydam and Cifelli, 2002).

Although the vast majority of turtles recovered from the Antlers Formation are represented by fragments (Cifelli et al., 1997; Joyce et al., 2011), a 1940s field expedition by the Field Museum of Natural History recovered a near-complete turtle skeleton at Triconodont Gully near Forestburg, Montague County, Texas (Fig. 1). The specimen, catalogued as FMNH PR273, is exceptionally preserved and was identified readily as the first known skeleton of *Naomichelys speciosa*, but it remains undescribed to date, perhaps because the cranium is the most poorly preserved portion of this exceptional skeleton. FMNH PR273 was nevertheless integrated into the phylogenetic analyses of Hirayama et al. (2000) and Anquetin (2012) and therein interpreted as a stem cryptodire or as a stem turtles, respectively, closely related to meiolaniid turtles. The shell was preliminarily figured by Hirayama et al. (2000), a limb with osteoderms was figured by Barrett et al. (2002), and the bone histology was investigated by Scheyer and Anquetin (2008). To date, FMNH PR273 is the only known solemydid specimen worldwide for which the limbs and vertebral column are known and for which the cranium and osteoderms were found in close association with a near complete shell. This specimen is therefore of great importance for the understanding of solemydid morphology and systematics.

The sole purpose of this contribution is to thoroughly describe the morphology of FMNH PR273 and to compare it with a select group of similarly sized and/or roughly coeval turtles. The phylogenetic relationships of this taxon will be explored elsewhere.

## METHODS

**Anatomical terminology.**—We herein follow the cranial and postcranial terminology as established by Gaffney (1972) and Gaffney (1990), respectively, but as modified for the carotid

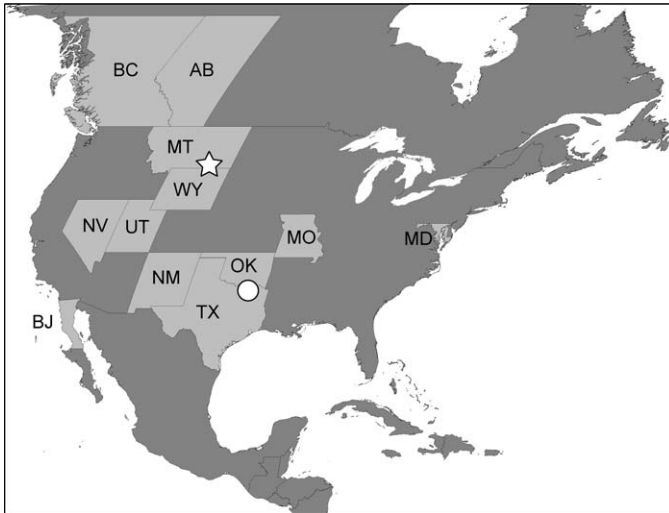


FIGURE 1—A simplified map of North America summarizing the reported distribution of Cretaceous turtle material referable to Solemydidae (as summarized by Joyce et al., 2011, with additions from Reynoso, 2006). The white star highlights the type locality of *Naomichelys speciosa*, the white circle the locality of FMNH PR273. Abbreviations: AB=Alberta; BC=British Columbia; BJ=Baja California; MD=Maryland; MO=Missouri; MT=Montana; NM=New Mexico; NV=Nevada; OK=Oklahoma; TX=Texas; UT=Utah; WY=Wyoming.

circulation system by Rabi et al. (2013) and for the plastral scales by Hutchison and Bramble (1981).

**Institutional abbreviations.**—AM, Australian Museum, Sydney, Australia; AMNH, American Museum of Natural History, New York, U.S.A.; DCM, Dorset County Museum, Dorchester, UK; FMNH, Field Museum of Natural History, Chicago, U.S.A.; MCZ, Museum of Comparative Zoology, Harvard University, Cambridge, Massachusetts, U.S.A.; MM, Mining and Geological Museum Sydney, New South Wales, Australia; MNA, Museum of Northern Arizona, Flagstaff, Arizona, U.S.A.; NHMUK (formerly BMNH), Natural History Museum, London, UK; NMB, Museum für Naturkunde, Berlin, Germany; NMS, National Museum of Scotland, Edinburgh, UK; PIN, Paleontological Institute of the Russian Academy of Science, Moscow, Russia; SMNS, Staatliches Museum für Naturkunde, Stuttgart, Germany; TMM, Texas Memorial Museum, Austin, Texas, U.S.A.; UCMP, University of California Museum of Paleontology, Berkeley, California, U.S.A.; UMZC, Cambridge University Museum of Zoology, Cambridge, UK; YPM, Yale Peabody Museum of Natural History, New Haven, Connecticut, U.S.A.

FMNH PR273 was photographed, illustrated, and described using traditional paleontological methods. In addition, however, the cranium was CT scanned at the facilities of the Department of Prehistory and Archeological Sciences of the University of Tübingen using a Phoenix v|tome|x. 729 slides were scanned at  $1068 \times 1382$  pixels and a resolution of  $100 \mu\text{m}$  per pixel. The resulting CT slices were primarily used to trace the path of circulatory and nerve canals within the basicranium.

We compare FMNH PR273 throughout the text to a select group of fossil turtles. Our sources are as follows.

Triassic turtles: *Proganochelys quenstedti* Baur, 1887 (as described by Gaffney, 1990; personal observations of material held at SMNS and NMB); *Palaeochersis talampayensis* Rougier, de la Fuente, and Arcucci, 1995 (as described by Sterli et al., 2007).

Early Jurassic turtles: *Kayentachelys aprix* Gaffney, Hutchison, Jenkins, and Meeker, 1987 (as described by Sterli and Joyce,

2007; personal observations of all material housed at MNA, MCZ, TMM, UCMP).

Middle Jurassic turtles: *Condorchelys antiqua* Sterli, 2008 (as described by Sterli and de la Fuente, 2010); *Eileanchelys waldmani* Anquetin et al., 2009 (as described by Anquetin, 2010; personal observations of all NMS type material); *Heckerochelys romani* Sukhanov, 2006 (as described by Sukhanov, 2006; personal observations of all type material held at PIN).

Late Jurassic turtles: *Dorsetochelys delairi* Evans and Kemp, 1976 (as described by Evans and Kemp, 1976; personal observations of type specimen held at DCM); *Glyptops plicatulus* (Cope, 1877) (as described by Gaffney, 1979; personal observations of AMNH 336 and YPM 1784); *Pleurosternon bullockii* (Owen, 1842) (as described by Evans and Kemp, 1975; personal observations of type specimen held at UMZC); *Xinjiangchelys qiguensis* Matzke et al., 2004 (as described by Matzke et al., 2004; personal observations of type specimen currently held at the University of Tübingen and likely soon transferred to the Paleontology Museum of Liaoning at Shenyang Normal University, Shenyang, China).

Cretaceous turtles: *Chubutemys copelloi* Gaffney, Rich, Vickers-Rich, Constantine, Vacca, and Kool, 2007 (as described by Gaffney et al., 2007; Sterli et al., in press); *Helochelydra nopcsai* Lapparent de Broin and Murelaga, 1999 (as described by Joyce et al., 2011; some shell and postcranial material is known for the holotype of *H. nopcsai* but remains undescribed); *Kallokibotion bajazidi* Nopcsa, 1923 (as described by Gaffney and Meylan, 1992; personal observations of all material held at NHMUK); *Mongolochelys efremovi* Khosatzky 1997 (as described by Khosatzky 1997; personal observations of all material held at PIN); *Patagoniaemys gasparinae* Sterli and Fuente, 2011 (as described by Sterli and Fuente, 2011); *Solemys vermiculata* Lapparent de Broin and Murelaga, 1996 (as described by Lapparent de Broin and Murelaga, 1996); *Spoochelys ormondea* Smith and Kear 2013 (as described by Smith and Kear, 2013; personal observations of specimens held at AM); *Tritinichelys hiatti* Gaffney, 1972 (as described by Gaffney, 1972; personal observations of type specimen held at MCZ).

Pleistocene turtles: *Meiolania platyceps* Owen, 1886 (as described by Gaffney, 1983, 1985, 1996; personal observations of all specimens held at AM and MM).

#### SYSTEMATIC PALEONTOLOGY

##### TESTUDINATA Klein, 1760

##### SOLEMYDIDAE Lapparent de Broin and Murelaga, 1996

##### NAOMICHELYS Hay, 1908

*Type species.*—*Naomichelys speciosa* Hay, 1908.

*Diagnosis.*—As for the type species.

##### NAOMICHELYS SPECIOSA Hay, 1908

##### Figures 2–20

*Type specimen.*—AMNH 6136, a partial entoplastron.

*Diagnosis.*—*Naomichelys speciosa* is referred to the clade Solemydidae based on the following combination of characters: lack of well-developed temporal emarginations; postorbital elongate; jugal does not contribute to orbit; squamosal expanded posteriorly; squamosal forms a triangular fossa at posterior margin of skull; pterygoids form an additional pair of tubercula basioccipitale; foramina pro ramo nervi vidiani (VII) visible in ventral view; osseous subdivision of ear cavity into a defined cavum acustico-jugulare and recessus scalae tympani absent; shell covered with sharply delineated, high tubercles that easily dislocate; entoplastron large, diamond-shaped and covered by entoplastral scute; anterior peripherals V-shaped in cross-section; limbs covered with osteoderms. *Naomichelys speciosa* primarily

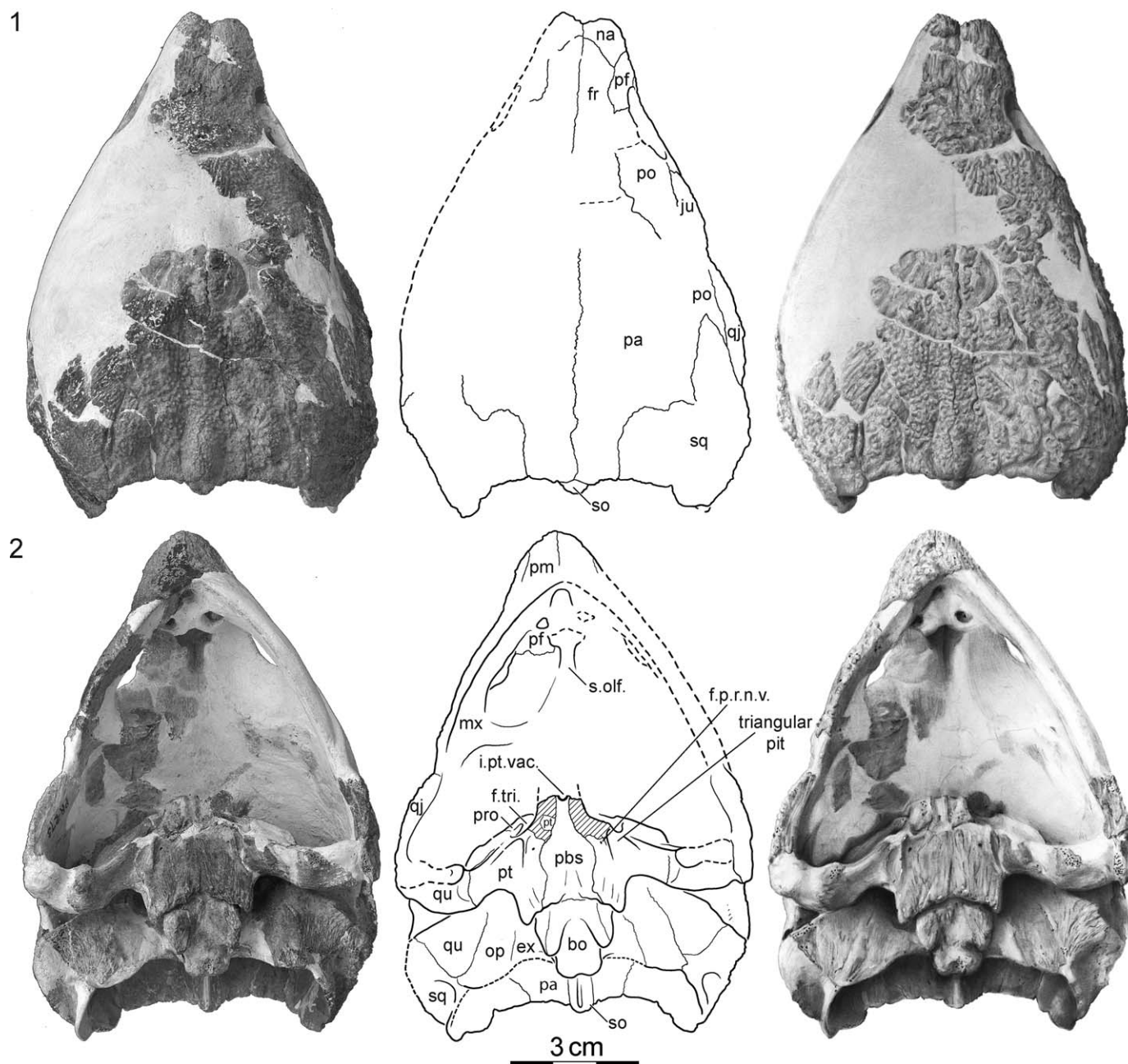


FIGURE 2—FMNH PR273, *Naomichelys speciosa*, from the Early Cretaceous (Aptian/Albian) Trinity Group of Texas, U.S.A. Photographs, line art, and shaded illustrations of skull: 1, dorsal view; 2, ventral view. Abbreviations: bo=basioccipital; ex=exoccipital; f.p.r.n.v.=foramina pro ramo nervi vidiani; f.tri.=foramen nervi trigemini; fr=frontal; i.pt.vac.=interpterygoid vacuity; ju=jugal; mx=maxilla; na=nasal; op=opisthotic; pa=parietal; pbs=parabasisphenoid; pf=prefrontal; pm=premaxilla; po=postorbital; pro=prootic; pt=pterygoid; qj=quadratojugal; qu=quadrate; s.olf.=sulcus olfactorius; so=supraoccipital; sq=squamosal. Shaded areas connote damage to the basicranial area, particularly the pterygoids.

differs from *Helochelydra nopcsai* by lacking pterygoids that fully cover the parabasisphenoid ventrally, by exhibiting an expanded symphyseal shelf, and by the unusual ventromedial folding of the coronoid process.

**Occurrence.**—Type locality “25 miles east of Pryor,” Montana, U.S.A. (Hay 1908, p. 101); Kootenai (Cloverly) Formation (Lower Cretaceous, Aptian) (Joyce et al., 2011).

#### DESCRIPTION OF FMNH PR273

**Cranium.**—Only about half of the skull of FMNH PR273 is preserved and is integrated into a reconstructive mount intended for exhibit (Figs. 2, 3). The reconstructed portions of the skull were not painted and it is therefore easy to distinguish between

reconstructed and authentic portions of the skull. Significant amounts of the dermatocranium are missing on the left side, but are preserved on the right side. The entire palatal region is lacking. Sutures are not clearly developed in many portions of the skull and often further obscured by plentiful cracks. We are therefore only able to reconstruct a limited amount of the morphology. A summary of select measurements is provided in the Appendix.

The skull of FMNH PR273 (snout to occipital condyle ~110 mm, see Appendix) is comparable to that of *H. nopcsai* (snout to occipital condyle ~100 mm) in general shape and size but differs by exhibiting more laterally oriented orbits and a more elongate

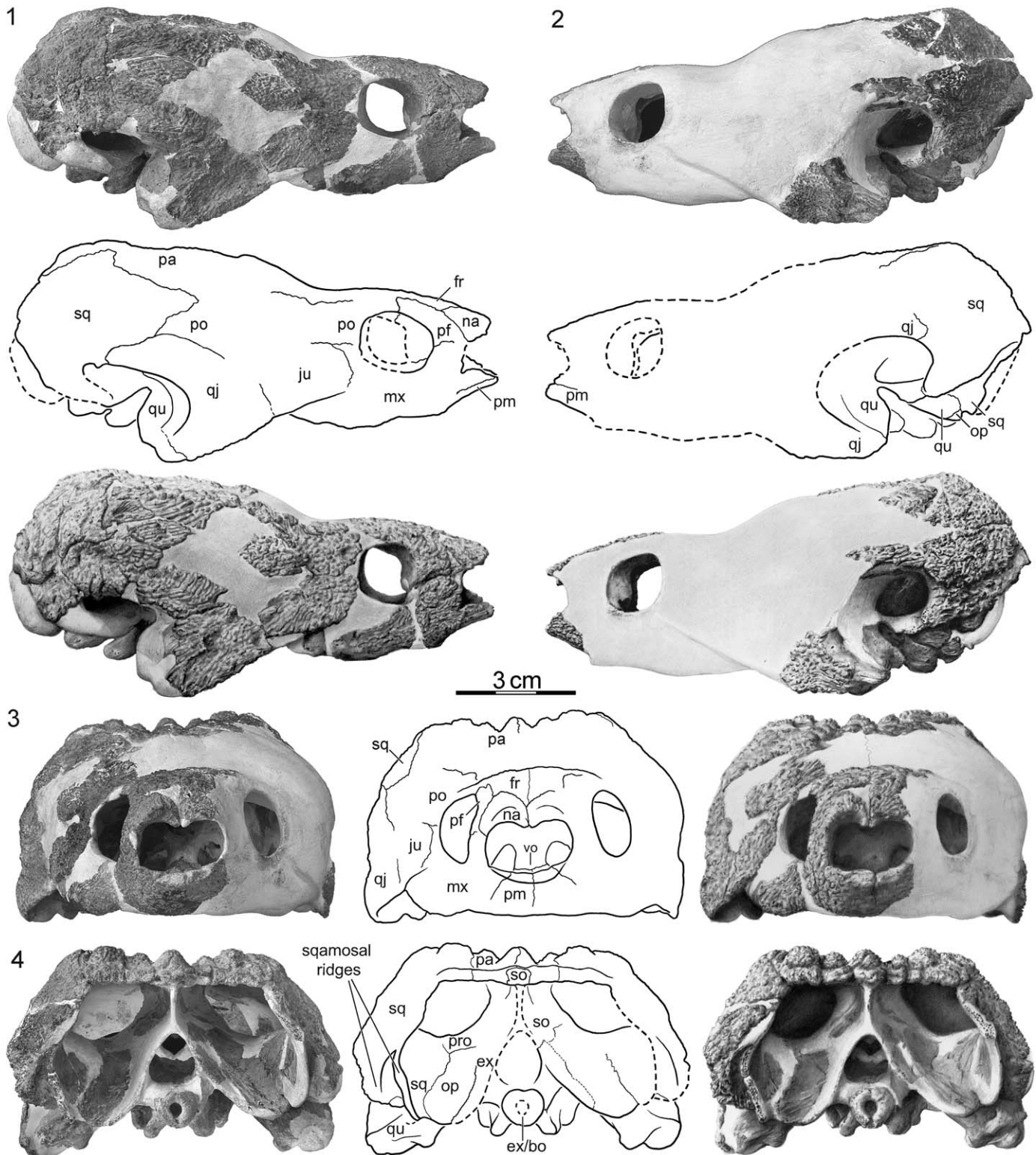


FIGURE 3—FMNH PR273, *Naomichelys speciosa*, from the Early Cretaceous (Aptian/Albian) Trinity Group of Texas, U.S.A. Photographs, line art, and shaded illustrations of skull: 1, right lateral view; 2, left lateral view; 3, anterior view; 4, posterior view. Abbreviations: ex/bo=exoccipital/basioccipital; fr=frontal; ju=jugal; mx=maxilla; na=nasal; op=opisthotic; pa=parietal; pf=prefrontal; pm=premaxilla; po=postorbital; pro=prootic; qj=quadratojugal; qu=quadrate; so=supraoccipital; sq=squamosal; vo=vomer.

snout (Figs. 2, 3). The entire skull surface is covered with low tubercles that resemble those of the shell but often coalesce. Among Jurassic and Early Cretaceous taxa, ornamentation on the dorsal surface of the skull is known for *Dorsetochelys delairi*,

*Pleurosternon bullockii*, *Glyptops plicatulus*, *Eileanchelys waldmani*, and *Heckerochelys romani*. However, the distinct pattern typical of solemydids is only apparent in FMNH PR273 and *H. nopcsai*. The dorsal surface of the parietal is notable in exhibiting

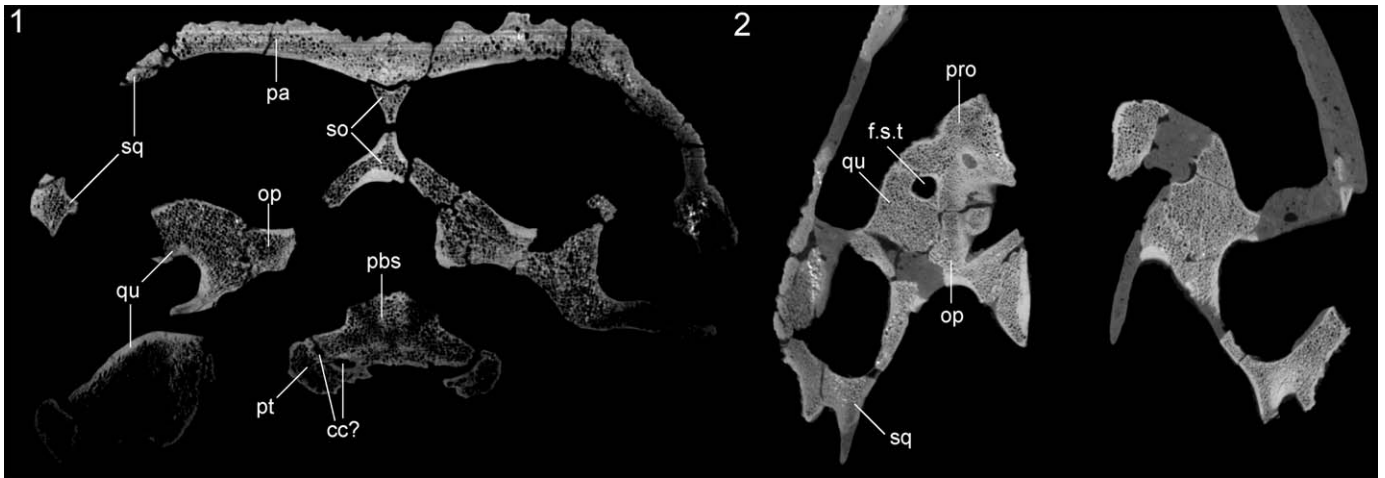


FIGURE 4—FMNH PR273, *Naomichelys speciosa*, from the Early Cretaceous (Aptian/Albian) Trinity Group of Texas, U.S.A. Sections of the skull produced using CT scans: 1, coronal section; 2, horizontal section. Abbreviations: cc=carotid canals; f.s.t.=foramen stapedio-temporale; op=opisthotic; pa=parietal; pbs=parabasisphenoid; pro=prootic; pt=pterygoid; qu=quadrate; so=supraoccipital; sq=squamosal.

a number of elongate protuberances that were likely covered by scales. The external nares are fully confluent. The lower temporal margin is slightly emarginated, but the upper temporal region is fully roofed. Sulcus like grooves can be found, particular along the posterior portion of the dorsal skull roof, but it is difficult to

trace them with confidence and establish a scute pattern, if present.

*Nasal.*—Both nasals are present, but the posterolateral portions of the left nasal are damaged (Figs. 2, 3). The dorsal exposure of the nasal is similar to that of the prefrontal and it is therefore

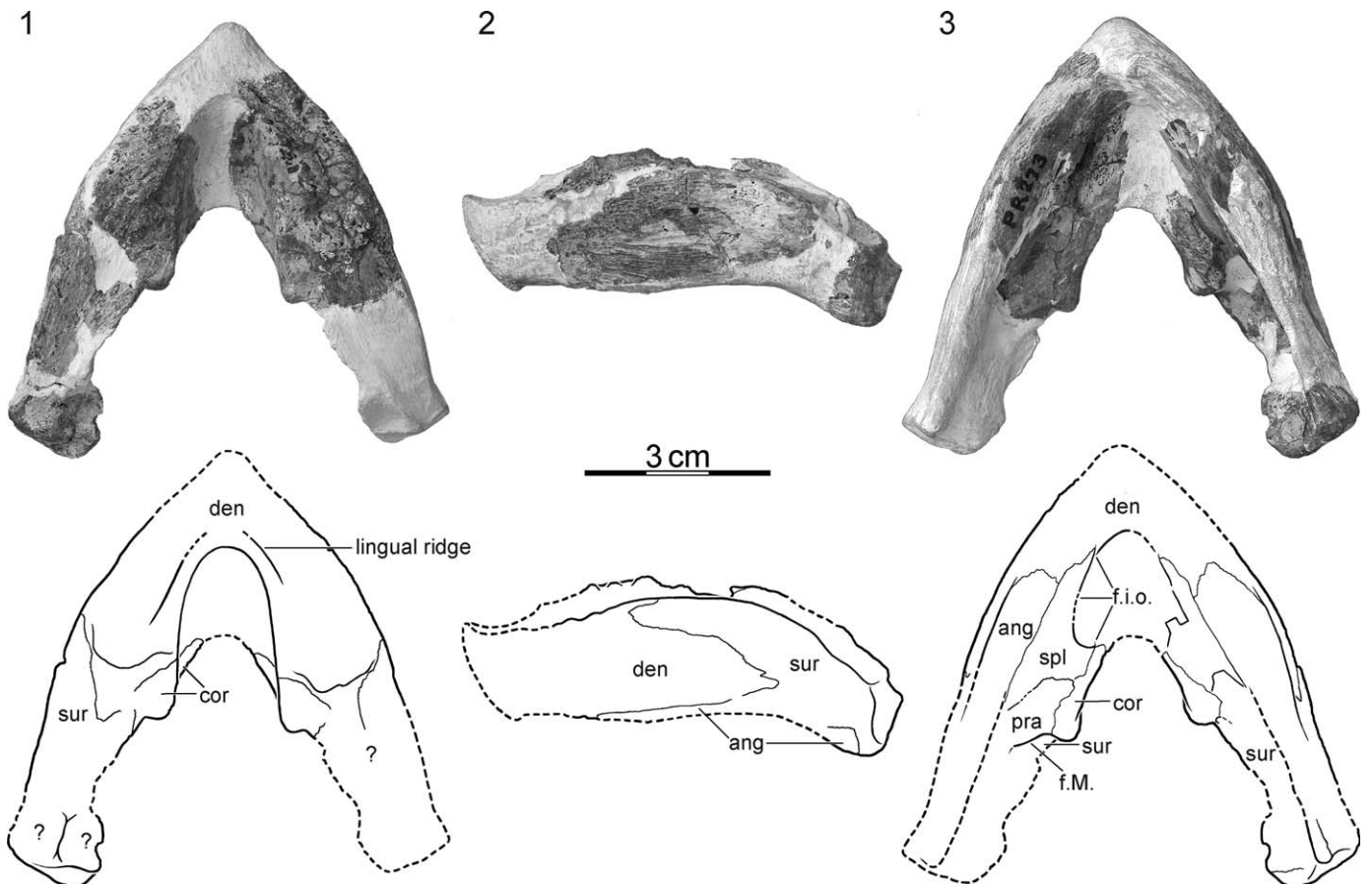


FIGURE 5—FMNH PR273, *Naomichelys speciosa*, from the Early Cretaceous (Aptian/Albian) Trinity Group of Texas, U.S.A. Photographs and illustrations of mandible: 1, dorsal view; 2, left lateral view; 3, ventral view. Abbreviations: ang=angular; cor=coronoid; den=dentary; f.i.o.=foramen intermandibularis oralis; f. M.=fossa Meckelii; pra=prearticular; spl=splenial; sur=surangular.

significantly larger relative to that of *H. nopcsai*. It is possible, however, that the anterior region of the skull of *H. nopcsai* is damaged and that the nasal region of these turtles is more similar than the specimen implies. The nasals contact one another along the midline, but the anterior processes of the frontals reduce this medial contact. The nasal contacts the frontal posteromedially and the prefrontal posterolaterally. The lateral aspects of the nasals are damaged and it is therefore unclear if they contacted the maxillae ventrolaterally. The nasals form a distinct groove along their midline contact, best seen from the anterior (Fig. 3.3), and form the dorsal aspects of the external nares. A small process is apparent along the narial margin of the nasal (Fig. 3.3) that may have supported a more extensive cartilage that subdivided the external narial passage.

**Prefrontal.**—The right prefrontal is preserved completely, but the left element is missing (Figs. 2, 3). The outline of the left prefrontal can nevertheless be partially reconstructed from the lateral margin of the left frontal. The dorsal exposure of the prefrontal is small, about equal to the dorsal exposure of the nasal. In dorsal view, the prefrontal contacts the nasal anteromedially, the frontal medially and posteriorly, the maxilla ventrally, and broadly forms the anterodorsal rim of the orbit as in *Kayentachelys aprix*, *E. waldmani*, *H. nopcsai*, *G. plicatulus*, *D. delairi*, and *Pl. bullockii*. It is unclear if the prefrontal contributed to the lateral margin of the external nares. The descending process of the prefrontal is well developed and helps to frame a broad fissura ethmoidalis (see frontals below). The end of the descending process is damaged and it is therefore unclear if a distal contact is present with the vomer and palatines. Within the orbit, the prefrontal contacts the frontal posteriorly and the maxilla ventrally.

**Frontal.**—The anterior portions of both frontals are well preserved, but damage to the skull obscures the posterior aspects of these bones (Figs. 2, 3). A transverse break on the right side of the skull is apparent crossing from the orbit to the midline of the skull (Fig. 2.1). This break may coincide with the posterior limits of the frontal and would imply that the frontal is L-shaped and much shorter relative to the elongate frontal of *H. nopcsai*. A short, linear structure is apparent further to the posterior, however, that also could be interpreted as the posterior suture of the frontal (Fig. 2.1). If correct, this position of the suture would imply an elongate, T-shaped element similar in shape and size to that of *H. nopcsai* and we therefore tentatively favor this interpretation. At the very least, the frontal contacts the nasal anteriorly, the prefrontal anterolaterally, contributes to the dorsal margin of the orbit, contacts the postorbital and parietal posteriorly, and broadly contacts its counterpart along the midline. Together with the prefrontals, the frontals form a key-hole shaped, but notably broad fissura ethmoidalis. The fissura is rounded dorsally at the end of the sulcus olfactorius and broadens ventrally (Fig. 2.2), in contrast to the condition seen in many testudinoids, in which the fissura is broadened dorsally (Joyce and Bell, 2004). Only the frontals contribute to the short, but distinct sulcus olfactorius. Further posteriorly a thickening to this bone highlights the lateral margin of the fossa orbitalis.

**Parietal.**—The parietals are the largest dermal roofing bones, but much of their anterior and lateral borders are unclear in dorsal view (Figs. 2, 3). The anterior contact with the frontal is most likely situated posterior to the orbits (see frontal for discussion). The anterior portion of the lateral contact with the right postorbital is well preserved, but obscured posteriorly by damage to the skull. The broad, sinuous posterolateral contact of the parietal with the squamosal is best preserved on the right side as well. The parietals broadly contact one another along the midline, share a short posterior contact with the supraoccipital, and contribute to the posterior margin of the skull. The dorsal skull roof of FMNH PR273 and *H. nopcsai* resembles that of *Proganochelys quenstedti*, *Condorchelys antiqua*, *K. aprix*,

*Spoochelys ormondea*, and *Chubutemys copelloi* by lacking upper temporal emarginations, but contrary to those taxa the posterior margin is mainly formed by the squamosals and not the parietals.

The ventral aspects of the parietals are damaged and obscured by the well-developed temporal roofing. It is nevertheless apparent that the parietals broadly contact the supraoccipital along an elongate anteroposterior suture in the posterodorsal region of the upper temporal fossa. In the anterior region of the upper temporal fossa, the parietals are damaged and the ventrally positioned bones with which they may have once been in contact are missing as well. It is therefore unclear if a descending process of the parietal was present.

**Postorbital.**—Only the right postorbital is present and its anterior and posterior borders are poorly preserved (Figs. 2, 3). The postorbital forms the posterior margin of the orbit and likely contacted the frontal dorsal to the orbit. The posterior portion of the postorbital bone is damaged and its posterior aspects are therefore unclear. However, by direct comparison to the skull of *H. nopcsai* it appears certain that the fragment of bone squeezed between the quadratojugal and squamosal is the postorbital. The posterior portions of the postorbital therefore broadly contact the parietal medially, the squamosal posteromedially, and the quadratojugal posterolaterally (Fig. 3.1). In ventral view, the postorbital exhibits a thickening that delineates the posterior margin of the orbital fossa. A notably elongated postorbital is always present in *E. waldmani*, *H. nopcsai*, *G. plicatulus*, *D. delairi*, and *Pl. bullockii*.

**Jugal.**—The right jugal is a rectangular element that does not contribute to the orbital margin, as in *H. nopcsai* (Figs. 2, 3). The jugal contacts the maxilla anteriorly and the quadratojugal posteriorly, but its dorsal and ventral contacts with the postorbital and maxilla, respectively, are partially obscured. It is therefore unclear if the jugal contributes to the lower temporal margin. The internal aspects of the jugal are not preserved.

**Quadratojugal.**—The right and left quadratojugals are damaged, but they combined document most aspects of this bone (Figs. 2, 3). The quadratojugal contacts the jugal anteriorly, but it is unclear if an anterior contact with the maxilla is present as well. The quadratojugal has a posterodorsal contact with the squamosal and likely had an anterodorsal contact with the postorbital (see above). Posteriorly the quadratojugal has a C-shaped contact with the quadrate. The anterior rim of the cavum tympani runs parallel and anterior to the quadrate suture. The posteroventral process of the quadratojugal extends to the level of the articular condyle and fully covers it in lateral view.

**Squamosal.**—The right squamosal is well preserved and primarily shows damage along its posterior margin (Figs. 2, 3). By contrast, only the posterior portion of the left squamosal is preserved. The squamosal is a large bone that covers much of the posterolateral aspects of the skull. The squamosal fully roofs the upper temporal fossa together with the parietal. The bone situated anterior to the squamosal is not clearly preserved on either side, but it appears likely that this region was filled with the postorbital, much as in *H. nopcsai* (see postorbital for discussion). The squamosal has a broad anteromedial contact with the parietal and a narrow ventral contact with the quadratojugal above the cavum tympani. The left squamosal reveals that this bone forms the posterodorsal margin of the rounded cavum tympani and the posterior aspects of the antrum postoticum and that it contacts the quadrate behind the incisura columella auris. In posterior view (Fig. 3.4), the squamosal has a broad contact with the paroccipital process of the opisthotic within the temporal fossa. More anterior contacts within the temporal fossa are not preserved. In posterior view, the squamosal forms a distinct ridge that merges dorsomedially with the posterior skull margin. This ridge splits ventrally into two poorly preserved ridges that define a triangular fossa that opens ventrally into the incisura columella auris. A

similar triangular fossa is also present in *H. nopcsai*. The squamosal expands posteriorly behind the posterolateral margins of the parietals, thereby forming much of the posterior border of the skull. This is also present in *H. nopcsai*.

**Premaxilla.**—The anterior portions of the premaxillae that form the snout are preserved, but significant portions are missing in the palatal region (Figs. 2, 3). The premaxillae combined form the ventral aspect of the steeply protruding nasal region, similar to that of *H. nopcsai*. Within the internal nares, the premaxilla broadly contacts the maxilla laterally and the vomer posteriorly and forms the ventral narial margin anteriorly. In anterior view (Fig. 3.3), the sutures are obscured towards the labial ridge, perhaps indicating that this individual was fully grown. It is nevertheless apparent that the premaxillae meet one another along the midline and posterodorsally contact the maxillae. In ventral view (Fig. 2.1), the premaxillae form the anterior portion of the labial ridge and form a deep midline pocket that may have provided space for a well-developed dentary hook. It is unclear if the premaxillae contributed to an extensive primary or secondary palate, as this region is not preserved.

**Maxilla.**—Only the anterior tip of the left maxilla is preserved along the lateral margin of the external nares (Figs. 2, 3). The right maxilla, by contrast, is more complete, but nevertheless lacks significant portions around the orbital margin and the entire palatal region (Figs. 2, 3). The maxilla contacts the premaxilla anteriorly and forms the lateral and ventrolateral portions of the external nares. In ventral view the maxilla forms a sharp labial ridge, but the shape and extent of the triturating surface are obscured by damage. The maxilla also contacts the prefrontal, and perhaps the nasal, dorsally, forming the anterior and ventral margin of the orbit. The broad posterodorsal contact of the maxilla with the jugal is somewhat obscured by a deep sulcus that may represent the margin of the rhamphotheca (Fig. 3.1, 3.2). It is unclear if the maxilla posteriorly contacted the quadratojugal, because the appropriate region is damaged. Any possible contact must have been minor, however, as in *H. nopcsai*.

**Vomer.**—Only the anterior tip of the vomer is preserved within the nasal cavity (Fig. 3.3). This fragment contacts the premaxilla anteriorly and the maxilla laterally. Potential contacts with the prefrontal, palatine, or other bones are not preserved.

**Palatine.**—The palatines are not preserved.

**Pterygoid.**—The anterior portion of the pterygoids is not preserved and numerous cracks in the basicranial region make it difficult to determine the limits of these bones with full confidence (Fig. 2.2). In ventral view, faint changes to the surface of the bone medially to the mandibular condyles indicate that the pterygoid forms a posterolateral process that is broadly sutured to the quadrate below the condylus mandibularis. The posterior process of the pterygoid laterally frames the parabasisphenoid complex. A direct posterior contact with the basioccipital, however, is hindered by a laminar gap. CT images reveal that one or two canals enter the skull within this gap (Fig. 4.1). The lateral of these two canals exits the skull and enters the cavum acustico-jugulare at the level of the incisura columella auris whereas the medial one cannot be traced with much confidence deeper inside the skull. Although it is likely that these vessels are associated with the cranial circulation, we are unable to confidently establish their homology, because of their unusual position and significant damage to the skull. We instead suggest that homology be established by direct comparison to *H. nopcsai* once CT scans are available for that taxon as well. The pterygoids form together with the basioccipital/exoccipital complex two pair of tubercula basioccipitale. This arrangement is otherwise only known for *H. nopcsai*.

The parabasisphenoid complex ends anteriorly along the midline in a semicircular notch with intact margins, which suggests the presence of a rudimentary interpterygoid vacuity. An anteromedial contact between both pterygoids cannot be

corroborated, as this region is not preserved. However, we presume that the pterygoids met one another along the midline anterior to this vacuity by direct comparison to *H. nopcsai*. It remains unclear if the palatine artery entered the skull within this vacuity.

A pair of triangular, posteriorly open pits is apparent along the base of the quadrate ramus, as in *H. nopcsai*. Small foramina are present just medial to these pits on both sides that again correspond closely to small foramina seen in *H. nopcsai*. We interpret these as the foramina pro ramo nervi vidiani (VII) by comparison to *G. plicatulus*, *Pl. bullockii*, and *Kallokibotio bajazidi*.

The dorsal contacts of the pterygoid are obscured by damage to the specimen. A large, anteriorly directed foramen and an anteriorly directed canal, best seen on the right side of the skull, are interpreted as the foramen cavernosum and the posterior portion of the trigeminal foramen, respectively. It is unclear if the trigeminal foramen is intact or if it used to be closed anteriorly by the descending process of the parietal.

**Epipterygoid.**—The epipterygoids are not preserved.

**Quadrate.**—The quadrates are present, but there is significant damage to both articular condyles and cava tympani (Figs. 2, 3). In lateral view, the quadrate forms a voluminous and confluent cavum tympani and antrum postoticum (Fig. 3.1, 2). The margins of the cavum, however, are formed by the quadratojugal and squamosal and the anterior margin of the antrum postoticum is not surrounded by the quadrate. The incisura columella auris is deep and fully open to the posterior. The quadrate contacts the squamosal posterodorsally and posteriorly and the quadratojugal dorsally and anteriorly to the cavum tympani.

Posterior to the incisura columella auris the quadrate forms a shelf in ventral view (Fig. 2.2) that broadly contacts the paroccipital process of the opisthotic medially along a near transverse suture and the squamosal posteriorly along an oblique suture, but the quadrate does not contribute to the posterior margin of the skull. Anterior to the incisura columella auris the quadrate broadly contacts the quadrate ramus of the pterygoid medially and the quadratojugal laterally. The articular condyles are badly damaged on both sides, but from what remains on the right side, it is apparent that the medial cotyle was well developed. Within the temporal fossa, the quadrate contacts the prootic anteromedially and contributes to the posterior margin of the trigeminal foramen (Fig. 3.4). Horizontally oriented CT images clearly reveal a large canalis stapedio-temporalis that is formed equally by the quadrate and the prootic (Fig. 4.2).

**Prootic.**—Portions of both prootics are preserved, but can only be observed partially in an oblique ventral view because the dermal roofing covers the dorsal view (Figs. 2.2, 3.4). The right prootic is better preserved than the left. This element contacts the quadrate laterally and the pterygoid ventrally. CT images reveal that the prootic and quadrate jointly form the large canalis stapedio-temporalis (Fig. 4.2). The likely dorsal contact with the parietal is not preserved. The prootic forms much of the dorsal aspects of the trigeminal foramen. The prootic forms a short anteromedially projecting process that partially or fully subdivided the trigeminal foramen into a dorsal and ventral aspect. The anterior margin of this process, however, shows evidence of damage and it is therefore unclear to what extent the subdivision of the trigeminal foramen occurred. The processus trochlearis oticum is formed entirely by the prootic. The posterior contact with the opisthotic is especially apparent in the CT images (Fig. 4.2).

**Opisthotic.**—The opisthotics are well preserved and show little damage (Figs. 2, 3). In ventral view (Fig. 2.2), the opisthotic contacts the quadrate anterolaterally along a transverse suture, contribute to the posterior margin of the skull, and broadly contact the exoccipitals medially. The inner ear is greatly

damaged and it is difficult to interpret the remaining structures. A low ridge is nevertheless apparent relatively deep within the otic region on the right part of the skull that we carefully interpret as the processus interfenestralis. The poor preservation of this process, however, precludes any further description. In posterior view (Fig. 3.4), the opisthotic contacts the quadrate laterally and the exoccipitals posteriorly. A short medial contact with the supraoccipital and an anterior contact with the prootic are apparent on the left side of the specimen. The posterior portion of the middle ear region is open and the foramen jugulare posterius is therefore fully confluent with the fenestra postotica. This region resembles that of *H. nopcsai*, *G. plicatulus*, *D. delairi*, and *Pl. bullockii*.

**Supraoccipital.**—The supraoccipital is badly damaged and the remaining fragments are held in the mount by large amounts of plaster (Figs. 2, 3). The supraoccipital forms a narrow crest that broadly contacts the parietals dorsally and that is barely visible along the posterior margin of the skull in dorsal view (Fig. 2.1). A small contribution of the supraoccipital to the skull roof is also present in *H. nopcsai*, *D. delairi*, and *Pl. bullockii*. The supraoccipital crest only protrudes slightly beyond the level of the occipital condyle, which is similar to the condition seen in *H. nopcsai*, *D. delairi*, *Pl. bullockii*, *Mongolochelys efremovi*, and *Trinitichelys hiatti*. The portion of the supraoccipital that likely roofed the foramen magnum is not preserved. With the exception of short posterolateral contacts of the supraoccipital with the opisthotic and exoccipital, all contacts are obscured within the temporal cavity (Fig. 3.4).

**Basioccipital and exoccipital.**—The exoccipitals and the basioccipital are fused into a complex indicating that the specimen is perhaps skeletally mature (Figs. 2, 3). The exoccipital portion is better preserved on the right side. The exoccipital forms part of the posterior margin of the skull, contacts the supraoccipital dorsally and opisthotic anterolaterally, and forms the lateral aspect of the foramen magnum. The occipital condyle has the shape of a strongly rounded triangle in posterior view (Fig. 3.4). However, the extremely deep “notochordal cavity” that is apparent in the center of the condyle is probably a human artifact to allow mounting the skull. The foramen jugulare anterius is present just posterior to the hiatus acusticus. As in *H. nopcsai*, the basioccipital/exoccipital complex and the pterygoids forms two pairs of tubercula basioccipitale, however, in FMNH PR273 the tubercula of the basioccipital/exoccipital complex are spaced more closely than those of the pterygoid and the depression defined by the tubercula is not as pronounced semilunate as in *H. nopcsai*. The basioccipital/exoccipital complex contacts the parabasisphenoid anteriorly along an anteriorly convex suture. An anterolateral contact with the pterygoids is hindered, however, by a laminar gap between these two bones.

**Parabasisphenoid.**—The parabasisphenoid is a flat bone that laterally contacts the pterygoid and posteriorly contacts the basioccipital/exoccipital complex (see above, Fig. 2.2). CT scans confirm that the surfaces of the parabasisphenoid are badly damaged. Anteriorly the parabasisphenoid forms the posterior margin of a slender interpterygoid vacuity. The anterior extension of the interpterygoid vacuity cannot be assessed with confidence because the relevant portion of the pterygoids is missing and it remains unclear if the palatine artery entered the skull at this point (Sterli et al., 2010). There is a pronounced step between the parabasisphenoid and pterygoids and between the parabasisphenoid and the basioccipital.

**Otic region and carotid circulation.**—The otic region shows some damage. From what is preserved, however, it is apparent that it greatly resembles that of the better-preserved *H. nopcsai*. The anterior regions of the middle and inner ear are damaged on both sides and an osseous subdivision of this space into a defined cavum acustico-jugulare or a recessus scalae tympani is either

missing or was never developed. Large openings are apparent for the canalis cavernosus and the canalis stapedio-temporalis. Joyce et al. (2011) interpreted a small opening anteroventrally to the hiatus acusticus of *H. nopcsai* as the foramen posterior canalis carotici interni, but this region is not preserved in FMNH PR273. We refrain ourselves from interpreting various foramina associated with the otic region because significant portions of the skull are missing and because those portions that are available imply a rather unorthodox arrangement of cranial vessels. A CT scan of the significantly better preserved skull of *H. nopcsai* is expected to provide much needed insights into the cranial circulation of solemydid turtles.

**Mandible.**—The mandible of FMNH PR273 is preserved, but significant portions are crushed or missing and were reconstructed with plaster, and many sutures are therefore difficult to discern (Fig. 5). The mandible is reconstructed as having a midline hook, but this area is not actually preserved. The deep pit visible in the triturating surface of the premaxillae (Fig. 2.2), however, may indicate that such a hook was indeed present. The mandible is highly unusual in its general morphology, because a broad shelf is developed along the symphysis, the triturating surfaces are extremely broad and low, the coronoid process is folded medially, and because the Meckelian canal system is fully obscured in dorsal view. The mandible is therefore primarily described in dorsal and ventral view.

**Dentary.**—The dentary is the largest bone of the mandible (Fig. 5). In dorsal view, the dentary exclusively forms the broad, low, but crenulated triturating surface. The labial margin is only weakly crenulated, but a well-developed, slightly serrated lingual ridge is apparent that is higher than the labial margin. In the plaster reconstruction, the ridge is reconstructed as forming a continuous U-shaped ridge, but there is no reason to believe this unusual arrangement was indeed present. In contrast to *H. nopcsai*, no pit is apparent in the posterior region of the triturating surface. The midline region of the jaw is missing and it is therefore not possible to determine if the symphysis was fused. The dentary forms a broad, midline shelf posterior to the symphysis. This shelf is thin and therefore cannot have supported much force. In dorsal view, the dentary contacts the coronoid posteromedially and the surangular posterolaterally.

In ventral view, the dentary forms the symphysis anteriorly, contributes to the bony symphyseal shelf, and contacts the angular and the splenial lateral to the foramen intermandibularis medius. The dentary also forms the dorsal roofing of the foramen intermandibularis medius and has a short contact with the coronoid medial to the horizontally flattened foramen. The broad posterior contact with the surangular is broadly developed in lateral view, but barely visible in ventral view.

**Angular.**—The angulars are poorly preserved in FMNH PR273, but enough remains to assert most of their morphology and contacts (Fig. 5). The angulars form the ventral aspect of the posterior two thirds of the mandible, as in *H. nopcsai*. The right angular is best preserved and shows a short anterior and a broad lateral contact with the dentary, and a broad medial contact with the splenial. The mid portions of both angulars are missing, but it is apparent in lateral view, that the angulars broadly contact the dentary and surangular dorsolaterally. The posterior tip of the left angular is preserved. It contributes to the posterior margin of the mandible, but given that all surrounding bones are fused, it is not possible to determine the posterior contacts.

**Surangular.**—The surangular of FMNH PR273 is highly unusual, because it forms not only the lateral aspects of the mandible, as in most turtles, but also the posterodorsal aspects anterior to the area articularis mandibularis, thereby covering the fossa Meckelii in dorsal view (Fig. 5). In dorsal view, the surangular contacts the dentary and coronoid anteromedially. The posterior contacts of the surangular are not clear and it is



uncertain if it contributed to the area articularis mandibularis. In lateral view (Fig. 5.2), the surangular contacts the angular ventrally and the dentary anteriorly along a broadly sinuous suture. The posterior contacts are again obscured. The surangular is broadly visible on the left side of the mandible in ventral view because the prearticular and splenial are missing. On the right side, by contrast, the surangular is only apparent posterior to the fossa Meckelii.

**Coronoid.**—Although both coronoids are preserved, significant damage to the surrounding bones obscures the contacts of the left coronoid. All observations are thus taken from the right side (Fig. 5). The coronoid is unusual because it is extremely low, lower than the lingual ridge, and because the coronoid process is directed posteromedially, instead of dorsally. Although it is possible that this unusual arrangement is a taphonomic artifact, we are confident that the mandible is not substantially deformed, because there are no signs of crushing, such as asymmetric cracks, and because the remaining skeleton shows no signs of crushing either. In dorsal view, the main body of the coronoid is situated posterior to the triturating surface and contacts the dentary anterolaterally and the surangular posterolaterally. The coronoid produces a small anteromedial process that is situated within the lingual groove and contributes to the symphyseal shelf that is formed by the dentary. In ventral view (Fig. 5.3), the coronoid forms much of the medial rim of the mandible. The anterior process closely approaches the foramen intermandibularis medius, but does not actually contribute to this foramen. The coronoid laterally contacts the splenial and the prearticular and posteriorly forms the medial rim of the horizontally oriented fossa Meckelii.

**Articular and area articularis mandibularis.**—Only the left articular is preserved, but its contacts with the surangular and prearticular are obscured by damage and/or fused sutures (Fig. 5). The area articularis mandibularis consists of two facets that are separated by a distinct anteroposterior ridge. The relative contributions of the surangular, articular, and prearticular to this structure are unclear. A short, rounded retroarticular process is developed posterior to the area articularis mandibularis.

**Prearticular.**—Only the anterior portion of the right prearticular is well preserved whereas the left is completely lacking (Fig. 5). The prearticular is oriented almost horizontally in this region and contacts the splenial anteriorly, the coronoid laterally, and forms the ventral rim of the fossa Meckelii posteriorly. All remaining contacts are not preserved.

**Splenial.**—There is substantial damage to the left splenial, but the right element is almost completely preserved (Fig. 5). The splenial is a flat bone that mediated between the vertical aspects of the ventral rim of the jaw and the horizontal aspects of the broad symphyseal shelf. In ventral view, the splenial contacts the dentary anteriorly, the angular laterally, the prearticular posteriorly, the coronoid posteromedially, and forms the entire ventral rim of the horizontally oriented foramen intermandibularis medius.

**Carapace.**—The carapace is generally well preserved, but localized damage is apparent that can be attributed to taphonomic crushing, weathering, and the recovery of the fossil (Fig. 6). Large portions of the nuchal, costals I, neural I, and the peripheral series are missing or were too poorly preserved to be included in the mount of the carapace. These portions were reconstructed in the mount and painted to have the same color as the surrounding bone. Much of this color was removed and the reconstructed portions highlighted prior to this study and the results therefore disagree slightly from previous studies (Hirayama et al., 2000; Anquetin, 2012).

The outline of the shell is that of an oval, with exception of a very deep anterior nuchal notch that is formed by the nuchal and peripherals I. The carapacial mount is reconstructed as having deep lateral gutters, but most of the relevant areas are not

preserved. However, a significant portion of the left peripheral series is preserved separated from the mount and confirms the presence of this gutter, even though it appears that diagenetic crushing exaggerated its extent. The gutter originates at the middle of peripheral III and continues around the posterior perimeter of the carapace. A number of basic measurements for the carapace are provided in the Appendix.

The entire surface of the carapace is covered with the raised pustules (Fig. 7) that are diagnostic for turtles of the clade Solemydidae (Lapparent de Broin and Murelaga, 1996, 1999; Joyce et al., 2011). The pustules range in diameter from 0.75 to 2 mm and are tall enough to dislodge easily from the surface of the shell. Towards the center of the carapace the pustules are low and narrow, closely spaced, and sometimes fused with one another in chains of up to four pustules. The costals are mostly covered with large, widely spaced pustules that only fused with one another occasionally towards the center of the carapace in pairs of two. The peripherals are covered with small, but widely spaced pustules. The pustules are arranged in a statistical pattern over the entire surface of the carapace and therefore show a pattern when viewed from a greater distance. It is apparent from the presence of sulci that the shell was systematically covered by scutes, but we have difficulties conjecturing how these scutes were attached to the skin, as no extant turtle has such an extreme surface texture. It is possible that the space between the pustules was covered by a thickened layer of skin and that the scutes therefore connected to the shell along a flat surface. It is furthermore possible that the scutes replicated the surface of the pustules thereby giving the scutes a rough surface that may have been useful as camouflage. Until the appropriate fossil evidence is available, we refrain ourselves from favoring any particular hypothesis.

At a broader scale, the shell is covered with domed structures that coincide with the distribution of the scutes (Fig. 6.3). All pleural scutes are surrounded by deep valleys and therefore have a broadly domed shape. Vertebrae II and III, by contrast, exhibit four humps each that are centered within the sinuous margins of these elements and vertebral IV possesses six such humps. A low, square midline keel is barely apparent on neural II and neural V–VIII.

**Nuchal.**—The nuchal is present, but partially damaged (Fig. 6). Only the median third of the anterior margin is authentic, whereas the two lateral margins are reconstructed in the mount. The posterior margin of the element is damaged as well and the detailed nature of the posterior contacts is therefore unclear. The external surface of what remains is well preserved, but much of the visceral surface is damaged.

The nuchal is a distinctly trapezoidal element that is approximately three times wider posteriorly than anteriorly, as in *Solemys vermiculata*, *Patagoniaemys gasparinae*, and *Mo. efremovi*. The anterior margin is characterized by a deep nuchal notch that is formed together with peripherals I, as in *S. vermiculata* and *Mo. efremovi*, among others. The nuchal contacts peripheral I anterolaterally, costal I posterolaterally, and neural I posteriorly. On the right visceral margin, a rib like process is apparent that likely corresponds to the neural crest derived, cleithral portion of the bone (Lyson et al., 2013). It is unclear if a blunt articular facet for articulation with the eighth cervical vertebra was present because the relevant portion of the nuchal is damaged. The right visceral side of the nuchal clearly documents that the anterior bridge cavity, which is mostly formed by the anterior peripherals, originates along the lateral margin of the nuchal. The visceral side of peripheral I is therefore split by the bridge cavity along its entire length.

**Neurals.**—Neural I is badly damaged, but the remaining portions of the neural series are well preserved (Fig. 6). There

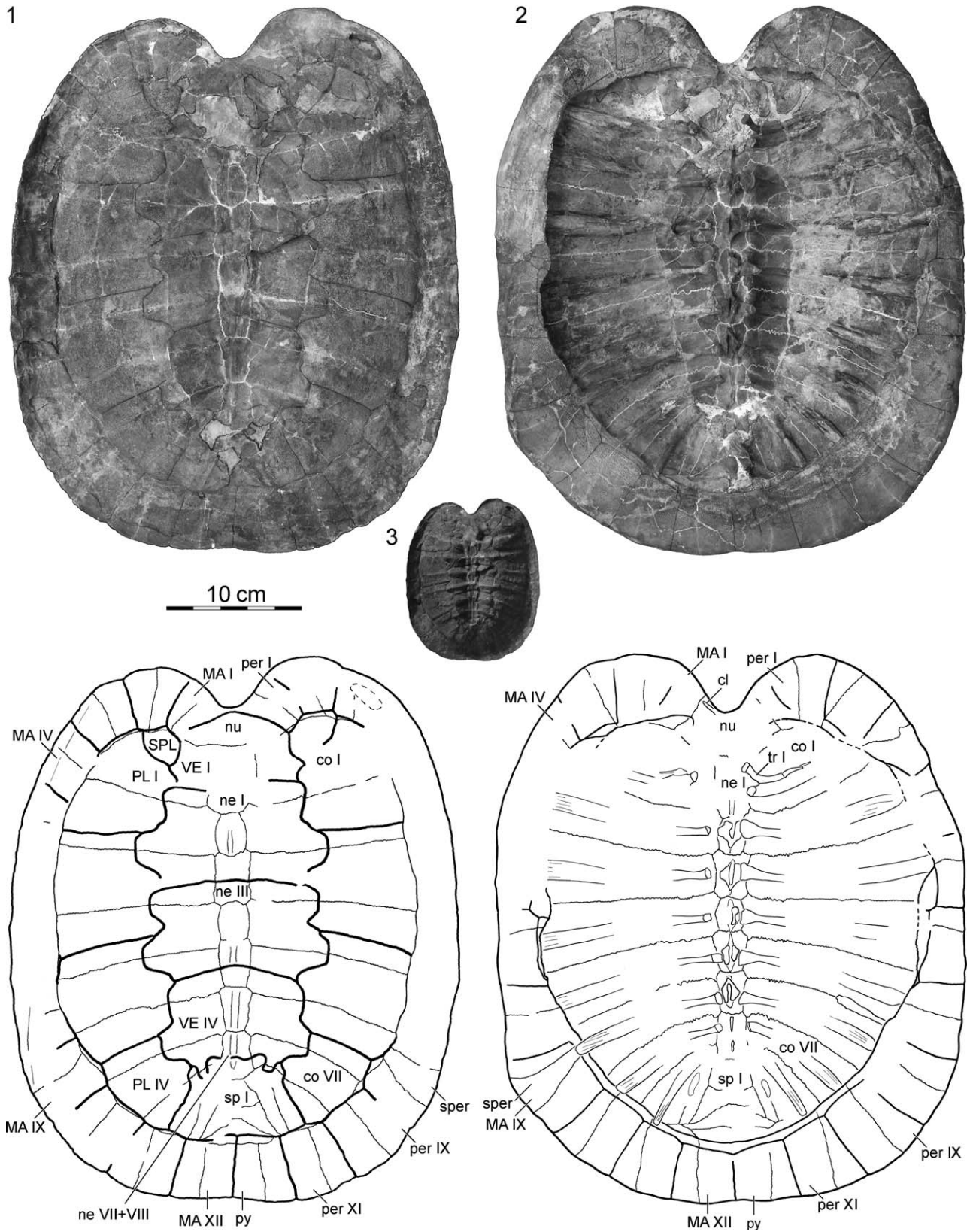


FIGURE 6—FMNH PR273, *Naomichelys speciosa*, from the Early Cretaceous (Aptian/Albian) Trinity Group of Texas, U.S.A. Photographs and illustrations of carapace: 1, dorsal view; 2, ventral view; 3, photograph of carapace in dorsal view taken with low light from the upper left highlighting three-dimensional shape of the scutes covering the specimen. Abbreviations: cl=cleithrum; co=costal; MA=marginal scute; ne=neural; nu=nuchal; per=peripheral; PL=pleural scute; py=pygal; SPL=supernumerary pleural scute; sp=suprapygal; sper, supernumerary peripheral; tr, thoracic rib; Ve=vertebral scute.

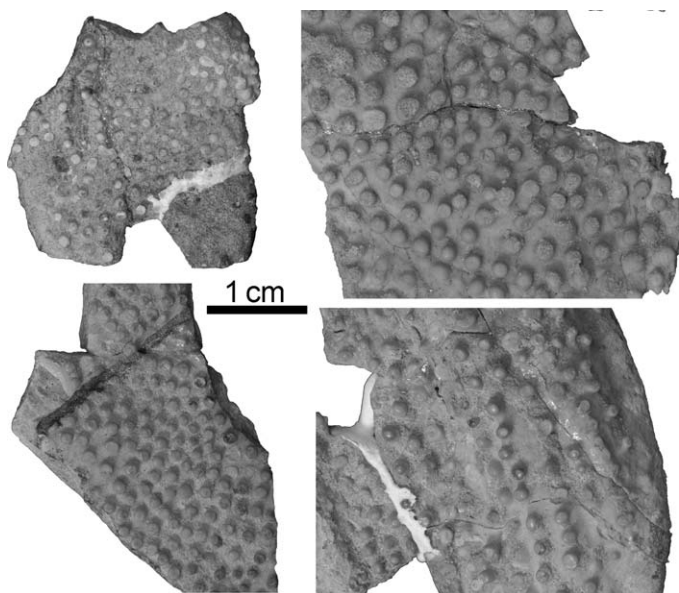


FIGURE 7—FMNH PR273, *Naomichelys speciosa*, from the Early Cretaceous (Aptian/Albian) Trinity Group of Texas, U.S.A. Photographs taken at the same scale highlighting variation in the surface sculpture of specimen.

is some apparent distortion to the region of neural I in the mount of the carapace and the proportions of neural I are therefore incorrect. However, it nevertheless appears certain that neural I is the longest and widest element of the neural series. Neural I anteriorly contacts the nuchal along a transverse suture, costal I along a parasagittal suture, and costal II and neural II along a posteriorly rounded, posterior suture. Although not preserved, neural I was crossed by the vertebral I/II sulcus. Neural II forms a small, rounded rectangle and is similar in size to the equally diminutive neural IV. Neural II contacts neurals I anteriorly, costals II laterally, and neural III posteriorly. A low, squared dorsal keel is apparent on this posterior portion of this element. Neural III is, after neural I, the second largest element of the neural series and was crossed by the vertebral II/III sulcus. It contacts three pairs of costals laterally, costals II–IV, and therefore has an octagonal outline. Neural IV resembles neural II in size and proportions and only contacts costals IV laterally. Neurals V and VI are elongate, hexagonal elements with short anterior sides. Both elements contact two pairs of costals laterally, are smaller than neural III, and are ornamented by a weak, squared, median keel. Neural V is crossed by the vertebral III/IV sulcus. A total of at least five elements are apparent posterior to neural VI. The posterior four of these lack neural arch attachment sites and are therefore interpreted as three small suprapyrgals and a large pygal. The most anterior element exhibits two neural arch attachment sites, is unusually large, and has an unusual polygonal shape for a single neural element. We therefore interpret this element as the fused neurals VII and VIII. The neural VII portion of the bone has a hexagonal outline with short anterior margins and represents the smallest element of the neural series. The neural VIII portion is slightly larger than neural VII, is hexagonal with short posterior sides, and contacts the most anterior suprapygal posteriorly. Neurals VII and VIII bear a weak, squared, median keel. Isolated neural bones of *S. vermiculata* also show the presence of this keel. The neural formula is  $6 > 4 < 8 > 4 < 6 < 6 | 6 >$ , where “<” and “>” indicate the placement of short sides. The complete neural series of *S. vermiculata* is unfortunately unknown. As in *Mo. efremovi*, neurals II and IV are small elements and only contact costals II and IV, respectively.

**Costals.**—The costal series is well preserved with exception of medial portions of costals I and VIII/IX (Fig. 6). The medial contacts of the costals with the neural series are described above. The costals clearly contact the anterior and posterior peripherals along sutures, but the nature of the lateral contacts is obscured in the mount. The medial aspect of the isolated left peripheral series, however, clearly demonstrates that not all costals and peripherals form sutural contacts with one another. Given how little space is available and that there is not evidence of free distal ribs, we presume that this animal did not possess well-developed carapacial fontanelles and that the costal and peripheral element simply abutted against each other in this region.

Costal I is the anteroposteriorly longest element of the costal series and significantly narrower mediolaterally than costal II. It contacts the nuchal, peripherals I and II, and the anterior portion of peripheral III anteriorly along sutural contacts, however, and the remaining contact with peripheral III and the anterior tip of peripheral IV appears to be a butt joint. Costals II–IV are the mediolaterally widest of the costal series and are mostly oriented transverse. Their lateral contacts with the peripherals are unclear, although it appears likely that each element was in contact with two peripherals. Costals V–VII gradually decrease in size and are more posteriorly oriented towards the back of the carapace. Costals V, VI, and VII laterally contact peripherals VII and VIII, VIII and IX, and IX and X, respectively, along sutural contacts. On the right side, costal VI furthermore contacts a slender, supernumerary peripheral. The most posterior costal element is partially separated by a suture that is visible in dorsal and ventral view and therefore appears to represent partially fused costals VIII and IX. In dorsal view, these elements combined contact neural VIII anteromedially, costal VII anterolaterally, the two anterior suprapyrgals medially, and peripherals X and XI posteriorly. These elements furthermore contact the most posterior suprapygal in visceral view. On the visceral side, the costal VIII portion of this bone is fully fused with costal rib IX. The costal IX portion, by contrast, only shows the attachment sites for costal ribs X.

**Peripherals.**—The peripheral series is generally well preserved, although significant portions of peripherals I and the bridge peripherals are missing or were too badly preserved to be included in the mount (Fig. 6). The right side is notable in that it exhibits a supernumerary peripheral that is squeezed between peripherals VIII and IX. This supernumerary element is generally shaped like the surrounding peripherals, but is significantly narrower anteroposteriorly. Its presence slightly reduces the size of the two neighboring peripherals, but does not change their contacts significantly by comparison to the other side of the specimen. The fully preserved left ventral side demonstrates that 11 pairs of peripherals are present. Peripherals I and XI contact the nuchal posteromedially and the pygal medially, respectively. The ventral contacts of the peripherals with the plastron are somewhat unclear, because this region is not preserved in articulation. However, a fragment of peripheral V that was left in articulation with the plastron together with the preserved bridge portions of the bridge peripherals allows assessing these contacts with some confidence. In particular, the hyoplastron, mesoplastron, and hypoplastron were in clear contact with peripherals IV and V, V and VI, and VI–VIII, respectively. The hyoplastron may have furthermore reached the most posterior limit of peripheral III, but this cannot be ascertained with any confidence. The remaining contacts with the costal are described above.

The visceral (or bridge) cavity, which is normally restricted to the bridge peripherals, is peculiar in that it extends anteriorly to the lateral margin of the nuchal. This morphology was previously noted for *S. vermiculata* (Lapparent de Broin and Murelaga, 1999). Cross sections of the anterior bridge peripherals are not

available and parts of this visceral cavity are either collapsed or filled with sediment. It is therefore not possible to confidently assess the nature of this cavity. However, a break to the dorsal surface of right peripherals II and III reveals that the visceral cavity tunnels below three quarters of these peripherals in this region. These peripherals therefore should approximate a V in cross section. The bridge peripherals are also deeply excavated and also mostly V-shaped in cross section. The bridge and the visceral cavity terminate half way along peripheral VIII. Posterior to the bridge region, the peripherals exhibit a thickened lip on the visceral side that parallels the scute/skin sulcus and the costoperipheral suture. A wide gutter is apparent that extends from the middle of peripheral III and that continues once around the entire posterior portion of the carapace. However, its morphology appears to be exaggerated by diagenetic crushing.

*Pygal and suprapygal.*—Four elements are present posterior to the neural series that are interpreted here as a single, large pygal and three suprapygals (Fig. 6). The pygal is slightly smaller than the surrounding peripherals and only contacts the third suprapygal anteriorly. It is fully integrated within the peripheral series and therefore forms part of the dorsal gutter and part of the visceral lip that parallels the scute/skin sulcus.

The first suprapygal is trapezoidal and roughly the size of the posterior neurals. The visceral side of this bone exhibit a weakly developed ridge that aligns with the broken off neural arch of thoracic vertebrae X. It is unclear, however, if a true connection was present. It would be reasonable nevertheless to interpret this element as a ninth neural. The second suprapygal has the shape of an inverted U and posteriorly surrounds and contacts the third suprapygal. This element otherwise contacts the first suprapygal anterior, costal IX anterolaterally, and peripheral XI posterolaterally. The third suprapygal is a lenticular element that contacts suprapygal II anteriorly and peripheral XI and the pygal posteriorly.

*Carapacial scutes.*—Even though the median portion of the nuchal is preserved, it is unclear if a cervical scute was present (Fig. 6). However, given that a midline sulcus is lacking that would indicate that the first two marginals contacted one another along the midline, it is apparent that this region was either covered by a single, awkwardly shaped midline element or that a cervical was present. Given the clear presence of cervicals in the closely related taxon *S. vermiculata* (Lapparent de Broin and Murelaga, 1999) we think it is more reasonable to speculate that a cervical was present.

Five wide vertebrals cover the median third of the carapace. All vertebrals are wider than the pleurals as in all basal turtles (Joyce, 2007). The first vertebral has a hexagonal shape with rounded margins. It contacts marginal I, and likely the cervical, along an anteriorly convex margin, the anterior supernumerary pleural, and pleural I along deeply convex lateral sulci, and vertebral II along a relatively straight transverse sulcus that traverses neural I. The sinuous lateral margin with the pleural series defines a pair of distinct carapacial humps. Vertebrals II and III are the widest vertebral elements. Both elements contact pleurals I and II along S-shaped anterolateral sulci and pleurals II and III along deeply convex posterolateral sulci, respectively. Centered within the convex portions of the lateral sulci, both elements exhibit two pairs of carapacial humps. The vertebral II/III sulcus transects neural III and the vertebral III/IV sulcus transects neural V as in most crown turtles (Joyce, 2007). Vertebral IV is narrower than vertebrals II and III, but wider than vertebrals I and V. Vertebral IV contacts pleurals III and IV along two S-shaped lateral sulci. The posterior sulcus with vertebral V is deeply sinuous and traverses neural VIII. Vertebral IV exhibits three pairs of carapacial humps that are centered within the convex portions

of this scute. Vertebral V is trapezoidally shaped and has dimensions similar to vertebral I. It contacts pleural IV along a rather straight sulcus laterally and the posterior half of marginal XI and all of marginal XII posteriorly.

The pleural series consists of four pairs of regular pleurals and a pair of anterior supernumerary pleurals (Fig. 6). The supernumerary scutes are asymmetrical, the right element being significantly larger than the left one. As a result, the large right supernumerary scute contacts marginals I–III anteriorly and blocks pleural I from contacting marginal II, whereas the small left supernumerary scute does not contact marginal III and thereby allows for a clear contact between pleural I and marginal II. The medial contact of the pleural series is described above. The lateral pleuromarginal sulcus corresponds closely to the costoperipheral suture. Pleural I may contact marginal II (see above) but otherwise contacts marginals III–V. The lateral contacts of pleural II are not preserved, but it can be inferred to have shared sulci with marginals V–VII. Pleural III contacted marginals VII–IX, and pleural IV marginals IX–XI.

*Plastron.*—The plastron is almost complete and the ventral surface is well preserved (Fig. 8). The anterior plastral margin, the left third of the entoplastron, and much of the visceral surface are damaged. The entire surface of the entoplastron is covered with the typical pustules that also cover the carapace (Fig. 7). The pustules along the central portion of the plastron are small and low. The pustules that cover the bridge, however, are significantly larger in all dimensions and resemble those on the peripherals. Only rarely do pustules fuse into groups of twos and threes. Some plastral measurements are provided in the Appendix.

The anterior rim of the anterior plastral lobe is damaged, it is nevertheless apparent that the anterior plastral lobe is about as long as the posterior plastral lobe, but wider at the base (Fig. 8). The entoplastron is a large element that almost fully spans the anteroposterior length of the anterior plastral lobe. It is diamond shaped and appears to have straight contacts with the surrounding bones. The visceral side of the entoplastron is badly damaged, the end of the blunt posterior plastral process and a semi-lunar elevated region are nevertheless apparent along the posterior half of this bone. See the Discussion below for a detailed comparison of the entoplastron of FMNH PR273 with the holotype of *N. speciosa* (AMNH 6136). The epiplastra are triangular elements that appear to only have a short contact anterior to the entoplastron. The brevity of this contact, however, may be exaggerated by the poor condition of the anterior plastral rim. In ventral view, the posterior contact of the epiplastron is a nearly transverse suture that is especially clear on the left side and different from the original interpretation painted onto the shell. Although somewhat obscured by poor preservation, it appears that the epiplastra/hyoplastral contact was deeply interfingered on the visceral side of the plastron. It is unclear if dorsal epiplastral processes were present, as the relevant area is poorly preserved.

The hyoplastra, mesoplastra, and hypoplastra contact one another along transverse sutures in ventral view and form the central portion of the plastron and the entire bridge region (Fig. 8). In visceral view, the hyoplastron and hypoplastron exhibit a number of finger-like processes that become more distinct towards the margins of each element. However, unlike the epiplastron/hyoplastron suture, these processes never lap onto the neighboring elements to form interfingering contacts. With exception of the posterior margin, the central plastral fontanelle is preserved intact and fully separates the mesoplastra long the midline. Much of the bridge contact is preserved, but the anterior plastral buttresses are damaged. It nevertheless is clear that the anterior plastral buttress was short, only in contact with peripherals, and may have barely reached the posterior edge of

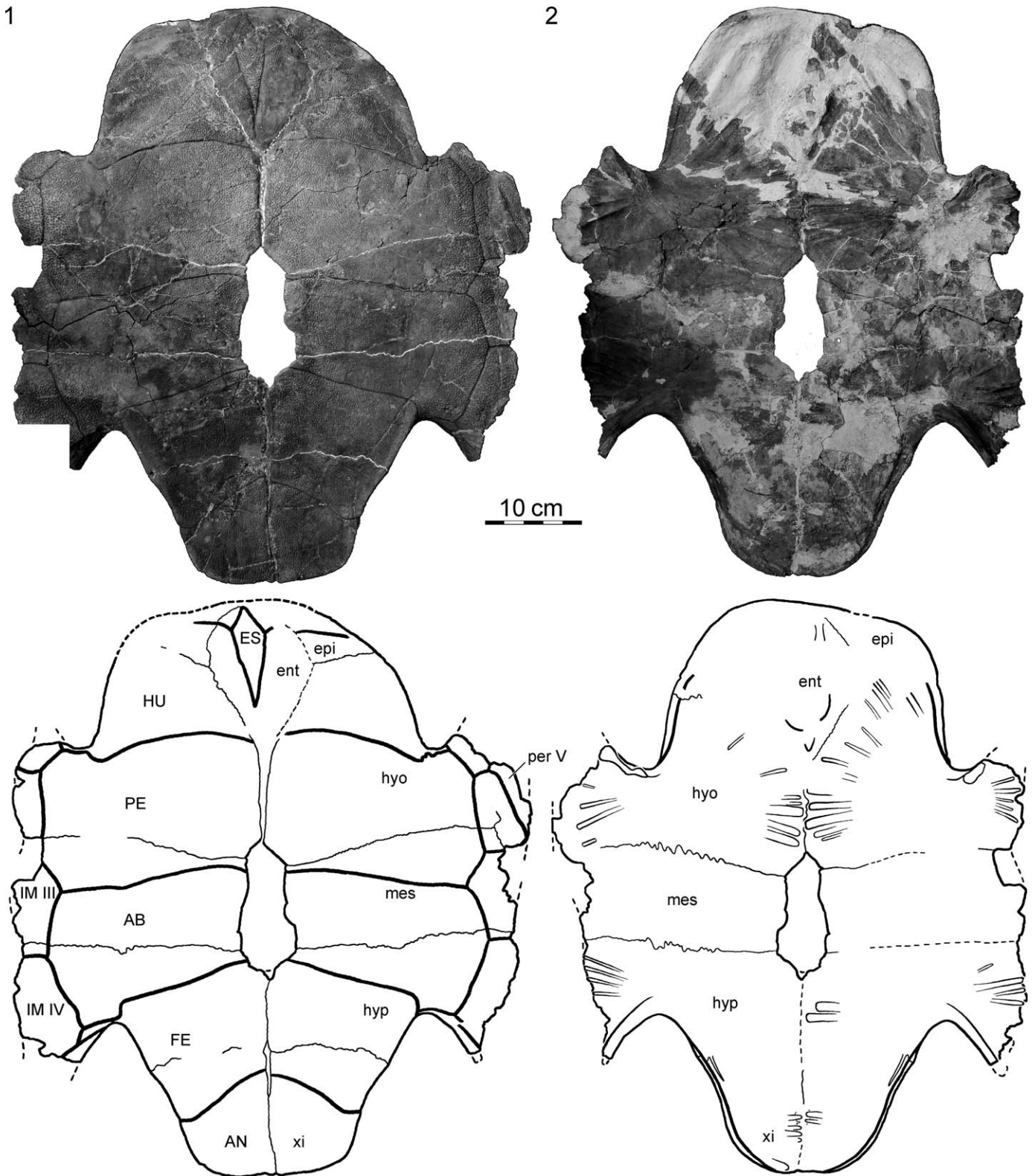


FIGURE 8—FMNH PR273, *Naomichelys speciosa*, from the Early Cretaceous (Aptian/Albian) Trinity Group of Texas, U.S.A. Photographs and illustrations of plastron: 1, ventral view; 2, dorsal view. Abbreviations: AB=abdominal scute; AN=anal scute; ent=entoplastron; epi=epiplastron; ES=entoplastral scute; FE=femoral scute; HU=humeral scute; hyo=hyoplastron; hyp=hypoplastron; IM, inframarginal scute; mes=mesoplastron; PE=pectoral scute; per, peripheral; xi=xiphiplastron.

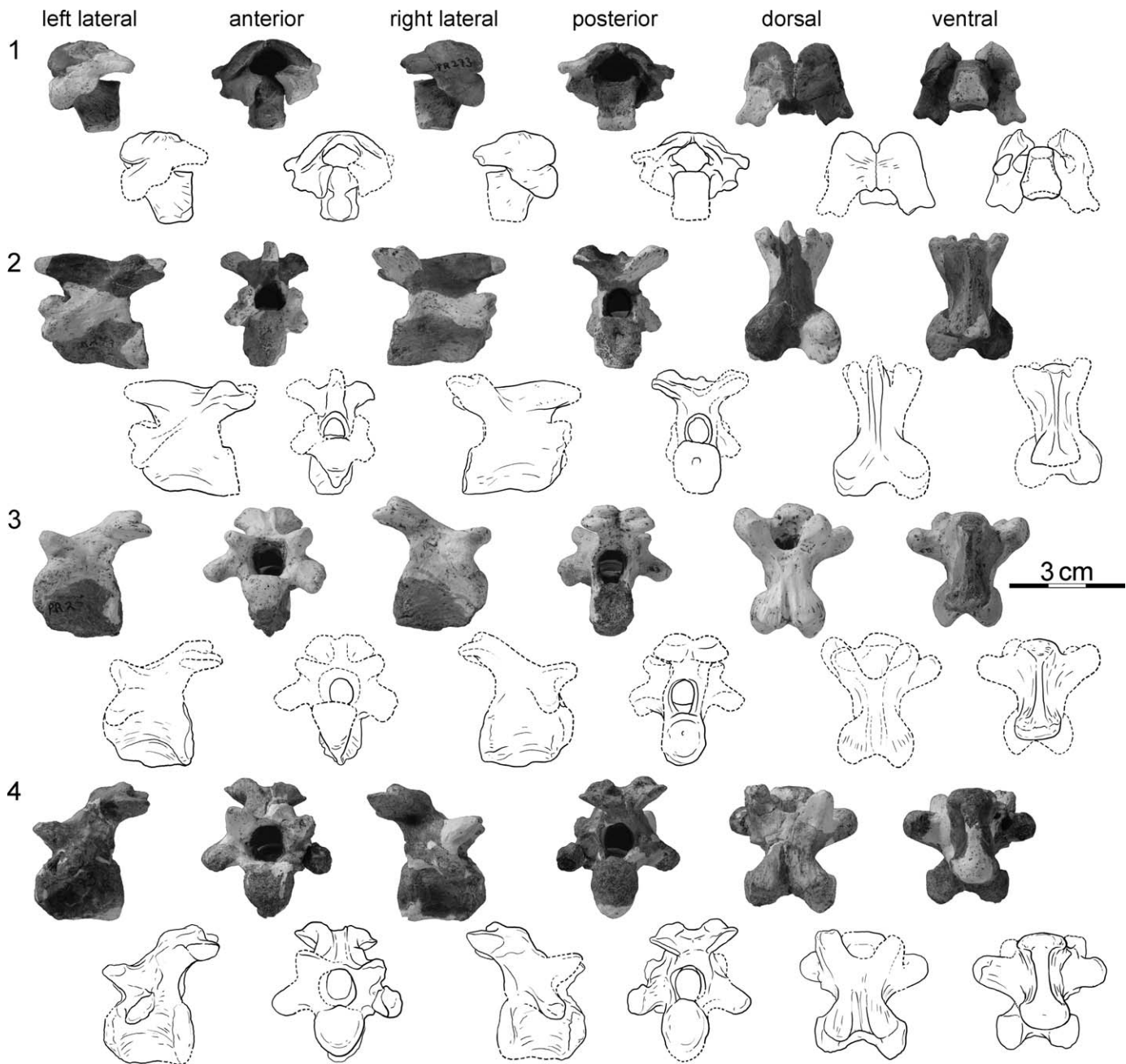


FIGURE 9—FMNH PR273, *Naomichelys speciosa*, from the Early Cretaceous (Aptian/Albian) Trinity Group of Texas, U.S.A. Photographs and illustrations of cervical vertebrae I (1), II (2), III (3), IV (4), V (5), VI (6), VII (7), VIII (8).

peripheral III. The posterior plastral buttress only forms a minor process that reached the middle of peripheral VIII. The lateral contacts with the peripherals are described above. Although the presence of a central plastral fontanelle is often seen as a sign of skeletal immaturity, many taxa are known to have central plastral fontanelles, even as adults (Hirayama et al., 2000). And given that the preponderance of available information hints towards the skeletal maturity of this specimen (e.g., fused exoccipital and basioccipital, poorly visible cranial scutes, tightly sutured glenoids and acetabula), we conclude that *N. speciosa* was characterized by a central fontanelle throughout its life.

The posterior plastral lobe has a transverse posterior margin (Fig. 8). An anal notch is absent. The hypoplastron and xiphiplastron contact one another in ventral view along a

transverse suture, but their visceral contact is mostly obscured, with exception of the deeply interfingered lateral portion. The xiphiplastron exhibits a number of finger-like processes, but they line up along the midline and do not form an interfingered contact.

*Plastral scutes.*—It is not possible to rigorously assess the number and contacts of gular elements due to significant damage along the anterior rim of the plastron (Fig. 8). A well-developed transverse humeral/gular sulcus across the middle of the epiplastron nevertheless indicates that at least one pair of gular scutes is present. A supernumerary midline element, termed the entoplastral scute by Lapparent de Broin and Murelaga (1999), is present. This elongate, diamond shaped element nearly spans the fully length of the entoplastron, narrowly contacts a gular element

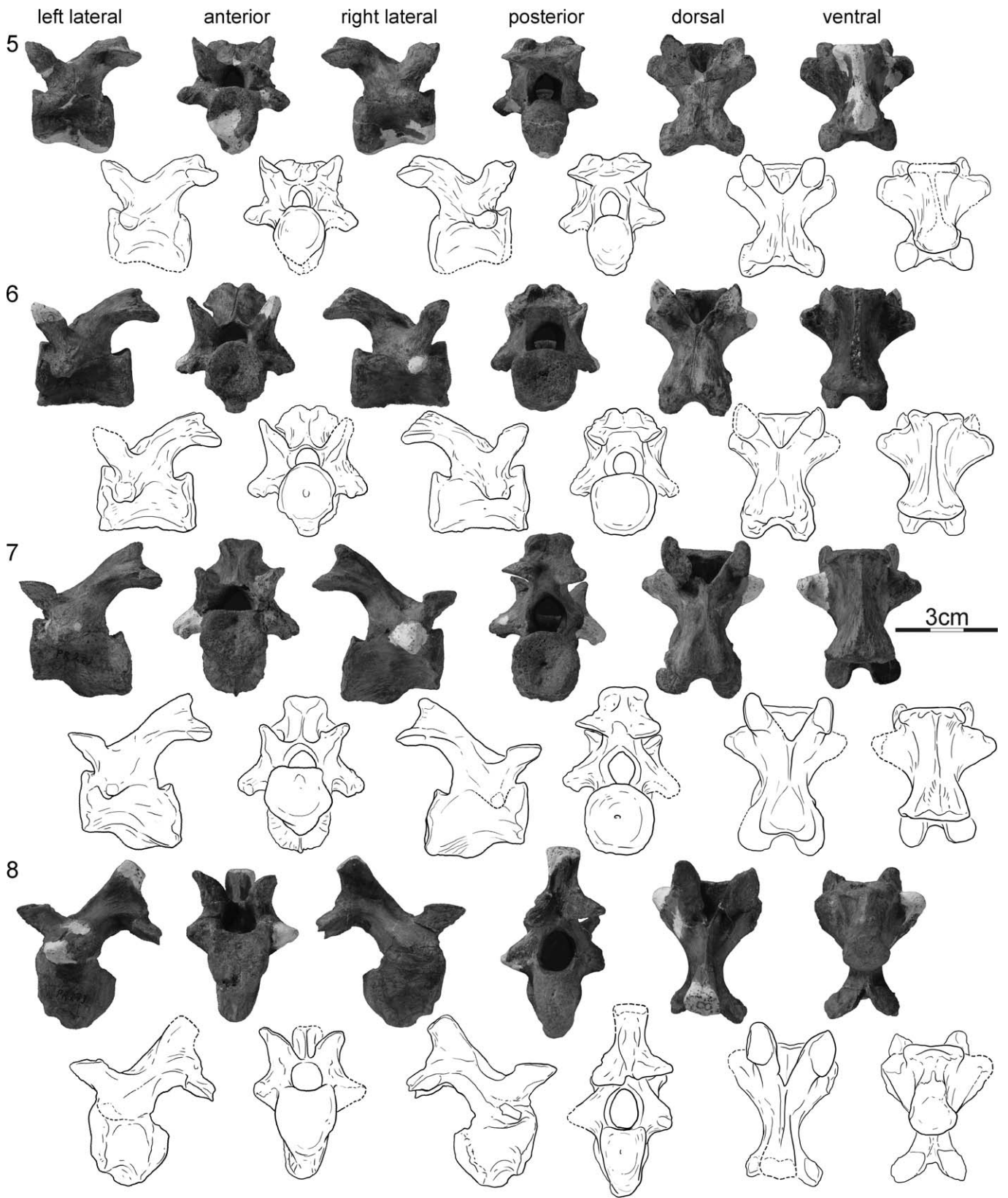


FIGURE 9—Continued.

anterolaterally and broadly contacts the humeral posterolaterally. Entoplastral scutes are otherwise known from *S. vermiculata*, *H. nopcsai*, and the holotype of *N. speciosa* (Hay, 1908; Lapparent de Broin and Murelaga, 1999). The humeropectoral sulcus is convex anteriorly, may have barely lapped onto the posterior tip of the entoplastron, and terminates laterally at an inframarginal. The pectoral/abdominal sulcus is convex anteriorly and located posterior to the hyoplastron/mesoplastron suture. The abdominal/femoral and femoral/anal sulci are also convex anteriorly and cross the hypoplastron and xiphoplastron, respectively. The plastral scutes lap a few millimeters onto the visceral side of the plastron and form a narrow dorsal lip. The bridge region is partially damaged on both sides of the plastron, but a continuous series of four inframarginals is nevertheless apparent. The pectoral scute contacts the anterior three inframarginals whereas the abdominal scute contacts the posterior two inframarginals.

**Cervical vertebrae and ribs.**—The cervical column is complete with exception of the atlas intercentrum (Fig. 9). All preserved cervicals show signs of damage and were partially restored with plaster for use in a mount. The ventral margin of the centrum and a portion of the left neural arch are damaged in the atlas. Cervical II, the axis, consists of two large pieces, part of the neural arch and part of the centrum, which are held together by plaster. Only parts of the centrum remain of cervical III. The remaining five cervicals are much better preserved: cervical IV mostly shows damage to the right prezygapophysis and the posteroventral margin of the centrum, cervical V only shows damage to the ventral ridge of the centrum, cervical VI is missing the anterior tip of the left prezygapophysis and the tip of the right diapophysis, whereas cervical VII is lacking the right diapophysis. Cervical VIII shows damage to both diapophyses and the tip of the dorsal process.

**Cervical ribs.**—It is apparent that FMNH PR273 must have represented a near complete skeleton when it was recovered from the field, because many small bones are present, such as osteoderms or phalanges. There is a notable lack of cervical ribs, however, dia- and parapophyses are present. This may either reflect a true absence of cervical ribs and thereby question the utility of using dia- and parapophyses in inferring the presence of cervical ribs (see Joyce, 2007) or may be the result of all cervical ribs having been collected in a single vial during the preparation process, much as other small bones were collected, and the vial having been lost in the last 60 years. Until additional material is collected, we cannot distinguish between both plausible hypotheses, although we think it to be more plausible that the cervical ribs were lost during recovery. Cervical ribs are rarely preserved, but appear to be plesiomorphically present in most basal turtles (Joyce, 2007).

**Atlas.**—The neural arches and centrum of the atlas are conjoined into a complex (Fig. 9.1). The anterior face of the atlas exhibits three dorsal and one ventral articular facet that are arranged in a T-shape. The ventral facet slopes posteriorly and serves as the articular surface for the atlas intercentrum, whereas the median of the three dorsal facets serves as the articular surface for the occipital condyle. The two lateral facets slope laterally and articulate, but do not fuse, with the neural arches. The atlas centrum expands dorsally and forms a high, slightly rounded rectangle in posterior view. The ventral portions of the centrum are damaged and were reconstructed with plaster.

The left atlas neural arch shows significant damage (Fig. 9.1) and this description therefore focuses on the near complete right element. The atlas neural arch consists of a massive ventral portion and a plate like dorsal portion. The ventral portion produces a medially sloping facet for articulation with the occipital condyle, medially contacts the centrum, and is dorsally connected with the dorsal portion of the neural arch. The ventral portion furthermore forms a posterolaterally directed process,

likely for muscle attachments, but the process broke off near its base. The dorsal plates arch over the neural canal, meet along the midline, but are not fused. Posterolaterally, the neural arches form a broad process. The medial aspect of this process serves as the ventromedially facing postzygapophysis whereas the lateral aspect forms a posterolaterally facing muscle attachment site.

**Cervical centra.**—The cervical centrum of the atlas is described in detail above. The anteroposterior length of the cervical centra gradually increases from anterior to posterior, with two exceptions: centrum II is longer than centrum V and centrum VIII shorter than centrum V. The cervical central lengths can therefore be summarized as  $I < III < IV < VIII < V < II < VI < VII$  (Fig. 9).

The centra exhibit an intermediate condition between the plesiomorphic amphicoelous pattern seen in basal turtles and the derived pattern with fully formed articulation seen in all extant turtles (Fig. 9). A number of vertebrae have articulations that are clearly concave, such as the posterior articulation of cervical I, or the anterior articulations of cervicals V and VI. Only the posterior articulation of cervical VIII is clearly convex, whereas others are only lightly so. A number of articulations, however, are rather poorly defined, and are addressed here at platycoelous. The cervical formula therefore is  $1( |2( ?3( (4) )5) )6| |7( |8)$ . This cervical formula is similar to that found in *Pat. gasparinae* or *Meiolania platyceps* by exhibiting a biconvex cervical IV, but by lacking the double joint seen in many extant cryptodires. The articulations between all cervicals are vertical or slope slightly to the anterior, with exception of the articulation between cervicals VII and VIII, which slopes strongly towards the anterior (Fig. 9).

The anterior and posterior articulations of cervicals II–VII are of equal size and the main body is reduced in width (Fig. 9.2–9.7). These cervicals are therefore strongly hourglass shaped in ventral view. The posterior articulation surface is much greater than the anterior one in cervical I and this element therefore expands in its width to the posterior (Fig. 9.1). The posterior articulation of cervical XIII is only half of the width of the anterior articulation (Fig. 9.8). This element therefore forms an hourglass with reduced posterior width. In anterior and posterior views, all articulations are either round to squarish to high-oval or high-rectangular. The articulations are never wider than high (Fig. 9.1–9.8).

Cervicals II–VIII have a ventral keel, but this keel is damaged in cervicals II–VI and therefore may have been more expansive (Fig. 9.2–9.8). The keel of cervical III is preserved sufficiently to reveal that it protrudes ventrally beyond the central articulations. What remains of the keel of cervical VI indicates that it ends anteriorly in a well-developed process that is situated below the anterior central articulation. The well-preserved, narrow keel of cervical VII forms a distinct posteroventrally projecting process. The keel of cervical VIII is small and confluent with a bulbous process situated below the posterior central articulation.

The rim of the anterior central articulations of numerous cervicals is slightly eroded (Fig. 9), but cervicals IV, VI, and VII show paired anterolaterally directed parapophyses, which likely reveal the former presence of cervical ribs (see above).

**Cervical neural arches.**—The neural arches of all cervicals continuously grow in height from anterior to posterior (Fig. 9). The neural arch of the atlas differs categorically from the rest and is described above. The neural arch of the axis, however, mediates between the atlas and the more posterior cervicals. Large portions of the axial neural arches are unfortunately missing. It is apparent from what remains that the neural arch of the axis forms a Y-shaped dorsal ridge. The anterior aspect of this ridge is not connected to the prezygapophyses, but the posterior aspects terminate in a pair of bulbous muscle attachment sites above the postzygapophyses.



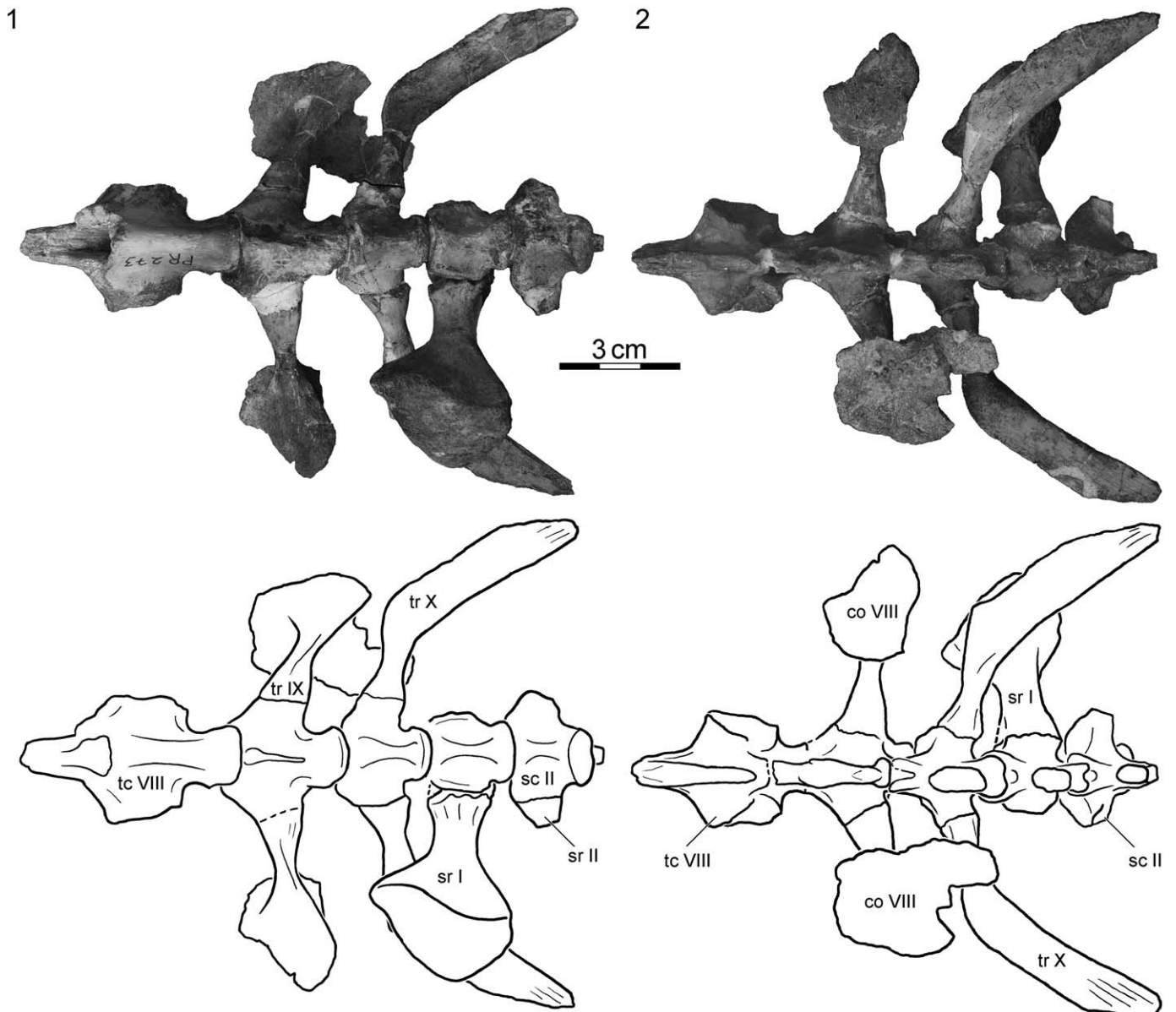


FIGURE 10—FMNH PR273, *Naomichelys speciosa*, from the Early Cretaceous (Aptian/Albian) Trinity Group of Texas, U.S.A. Photographs and illustrations of sacrum: 1, ventral view; 2, dorsal view. Abbreviations: co—costal; sc—sacral centrum; sr—sacral rib; tc—thoracic centrum; tr—thoracic rib.

Transverse processes are lacking in cervical I and not preserved—if present—in cervicals II and III (Fig. 9). The transverse processes of cervicals IV–VII are well preserved at least on one side of each vertebra. The processes, however, are broken on both sides of cervical VIII and they may therefore have been much more extensive originally. The processes are all well-developed, thick protrusions that are situated slightly anterior to the midline of the centrum as in *Pat. gasparinae*, *Me. platyceps*, and *Mo. efremovi*. The transverse processes of cervicals IV and V are slightly oriented to the anterior, but the remaining ones are oriented laterally. Small crenulations are apparent on all processes that likely served as muscle attachment sites.

The prezygapophyses are only preserved for cervicals IV, V, VII, and VIII (Fig. 9). These articular surfaces are well developed in all of these vertebrae, grow in size towards the posterior and are widely separately from one another. The prezygapophyses of cervicals IV and V face obliquely dorsally, medially, and

posteriorly. By contrast, those of cervicals VII and VIII face mostly dorsally and only slightly medially.

The postzygapophyses are preserved in cervicals II and IV–VIII (Fig. 9.2–9.8). As in all basal turtles, the postzygapophyses are situated on a well-developed posterior process. The postzygapophyses, however, are never confluent with one another. The postzygapophyses increase in size from the anterior cervicals to the posterior cervicals and their orientations correspond to those of the prezygapophyses they articulate with (see above). The postzygapophyses of cervical VIII are unusual in that they form an arch in lateral view and therefore face slightly anteriorly at their distal tips, a state reminiscent to that of extant cryptodires. Well-developed, posterodorsally oriented processes are apparent on top of the postzygapophysis, as in *Pat. gasparinae* and *Me. platyceps*. Towards the posterior, these processes become better developed, more separated from the underlying postzygapophyses, and more tightly spaced. The dorsal tip of cervical VIII is not preserved.

*Thoracic vertebrae and ribs.*—Although most of the thoracic vertebral column was likely present when the specimen was recovered from the field, only the three posterior elements are preserved and remain in articulation with the sacral column (Figs. 6, 10). Significant portions of the neural arches, however, remain associated with the neural series and reveal that each neural is connected with a single neural arch. The presence of two neural arches on the fused posterior neural element supports our assertion that this element represents fused neurals VII and VIII. Although speculative, it appears that costal ribs II–VII were in articulation with two centra. Costal ribs VIII–X, by contrast, demonstrably contact a single centrum only. This contrasts the condition seen in *Pat. gasparinae* where thoracic ribs II to X articulate with two thoracic vertebrae. Thoracic vertebra IX is platycoelous anteriorly and posteriorly, whereas thoracic vertebra X is platycoelous anteriorly and convex posteriorly, as in most turtles.

Much of the thoracic ribs are preserved in the carapacial mount (Fig. 6). Thoracic rib I is completely missing on the right side and only a short scar remains. However, the proximal two thirds of this rib is present on the left side indicating that this element spanned at least two-thirds the length of thoracic rib II, but only shared a short contact with it. A similar morphology is apparent in other basal turtles, such as *H. romani*. Thoracic ribs II–IX resemble those of most other turtles by having short proximal heads and by distally inserting bluntly into the peripheral series. The exact nature of the distal insertion is often unclear, however, because this area is often obscured by plaster. Thoracic rib X is preserved with the sacral column (Fig. 10). This rib is approximately half as long as thoracic rib IX and appears to have only been loosely associated with the costals, as it disarticulated from the shell at some point during its taphonomy. An attachment site for this rib is nevertheless apparent on the visceral side of the costals VIII/IX.

*Sacral vertebrae and ribs.*—The sacrum of FMNH PR273 consists of two vertebrae and is partially preserved in articulation with the posterior three thoracic vertebrae (Fig. 10). The centra are both procoelous, have an hourglass-shaped ventral ridge, and small, blunt dorsal processes. The pre- and postzygapophyses are well developed and resemble those of the anterior caudal vertebrae.

Only the right sacral rib I is preserved (Fig. 10). It is a large, block-like element that medially articulated at the middle of the sacral centrum I. Sacral rib I expands greatly distally, both in height and anteroposterior length and thereby gains the outline of a rounded triangle in lateral view. Only the medial portion of the right sacral rib II remains in articulation with its corresponding centrum. A blunt facet, however, is available along the posterior margin of sacral rib I for articulation with sacral rib II.

*Caudal vertebrae and ribs.*—The tail of FMNH PR273 was presumably complete when the specimen was recovered from the field, but some portions are now absent and were replaced by plaster (Fig. 11). The anterior portion of the tail is represented by three well-preserved caudals. The mid portion of the tail is represented by a string of 13 caudals, however, they do not articulate with caudal III. For purpose of mounting the specimen for museum display, a plaster vertebra was created that links the anterior and mid portions of the tail. We herein assume that this single vertebra was created, because a single vertebra was known to be missing and we number the caudal accordingly. The posterior end of the tail is completely recreated using plaster and is therefore omitted from the description. The tail therefore consists of at least 17 vertebrae, but the number was likely much greater. Many vertebrae are in articulation with neighboring elements and may show signs of reconstruction using plaster and paint.

The caudal centra continuously decrease in width and anteroposterior length towards the posterior (Fig. 11). All caudal centra are amphicoelous, as in the basal turtles *Pr. quenstedti*, *Palaeochersis talampayensis*, and *Condorchelys antiqua*, and lean slightly to the anterior in lateral view. All preserved caudals have transverse processes. The anterior six are about equal in width, but the posterior processes decrease quickly in size. The anterior six caudals lack attachment sites for chevrons. Although the chevrons are missing, caudals VII–IX exhibits well-developed attachment sites. The remaining caudals are all preserved in articulation with short, posteroventrally-oriented chevrons.

The anterior five caudals possess dorsal processes, which diminish in size towards the posterior and are barely noticeable on caudal V (Fig. 11). Widely spaced prezygapophyses are clearly developed on all vertebrae and are mostly oriented dorsomedially. The postzygapophyses resemble those of the cervicals, in that they are outgrowths of a posterodorsally projecting process. The postzygapophyses become more tightly spaced towards the posterior, but never become confluent.

*Pectoral girdle.*—The right and left scapulacoracoids are both preserved and only show minor damage (Fig. 12). The scapular process of the left scapulacoracoid, however, is fully replaced by plaster. The scapulacoracoid resembles that of most derived turtles in being a triradiate element, but it is significantly more robust than in most crown turtles. The scapula and the coracoid are tightly sutured one with another at the glenoid, but the elements are not fused. The neck of the glenoid is short, as in the vast majority of turtles. The scapular and acromial processes of the scapula are rod-shaped, distally striated, slightly oval in cross section, and connected by a low bony ridge. Distinct ridges that connect these two processes to the glenoid are absent. The scapular process is longer than the acromial process and the angle between them is approximately 100°. The coracoid is the shortest process and resembles that of meiolaniids and testudinids by having a narrow proximal shaft and by expanding distally to a semi-lunate plate. The distal margins of this plate are slightly thickened and show evidence of a cartilaginous cap. Distinct ridges that run from the acromial process to the glenoid are absent.

*Pelvic girdle.*—The pelvic girdle is generally well preserved, with exception of some damage to the descending branch of the right pubis, the distal end of the left ilium, and both acetabulae (Fig. 13). The right pelvis is better preserved in lateral view and the left pelvis in medial view. We therefore chose to figure these elements in those orientations (Fig. 13). The relatively low height of the pelvic girdle and the horizontal orientation of the dorsal edge of the ilium confirm that the shell of FMNH PR273 was low domed to flat. The exact outline of the acetabulum is uncertain, because this region is damaged on both sides. It is apparent, however, that all bones joined one another along tight, sometimes interdigitated sutures, but did not fuse into a solid element. In comparison to many other turtles, however, the acetabulum is notably massive relative to the surrounding bony projections.

The ilium generally resembles that of crown group cryptodires in having a stout, vertically oriented shaft and a dorsal fan that expands mostly towards the posterior (Fig. 13). The dorsal fan is striated along its medial and lateral sides. The ilium contacts the pubis anteroventrally and the ilium posteroventrally in the region of the acetabulum and was likely in contact with two pairs of sacral ribs.

The pubis and ischium also match with the general pattern seen in extant cryptodires by forming two pairs of processes with which the pelvis articulates with the plastron, the broad, anterolaterally directed lateral pubic processes, and the narrow, posterolaterally-directed lateral ischial processes. The lateral ischial processes are narrow and long as in *Xinjiangchelys*

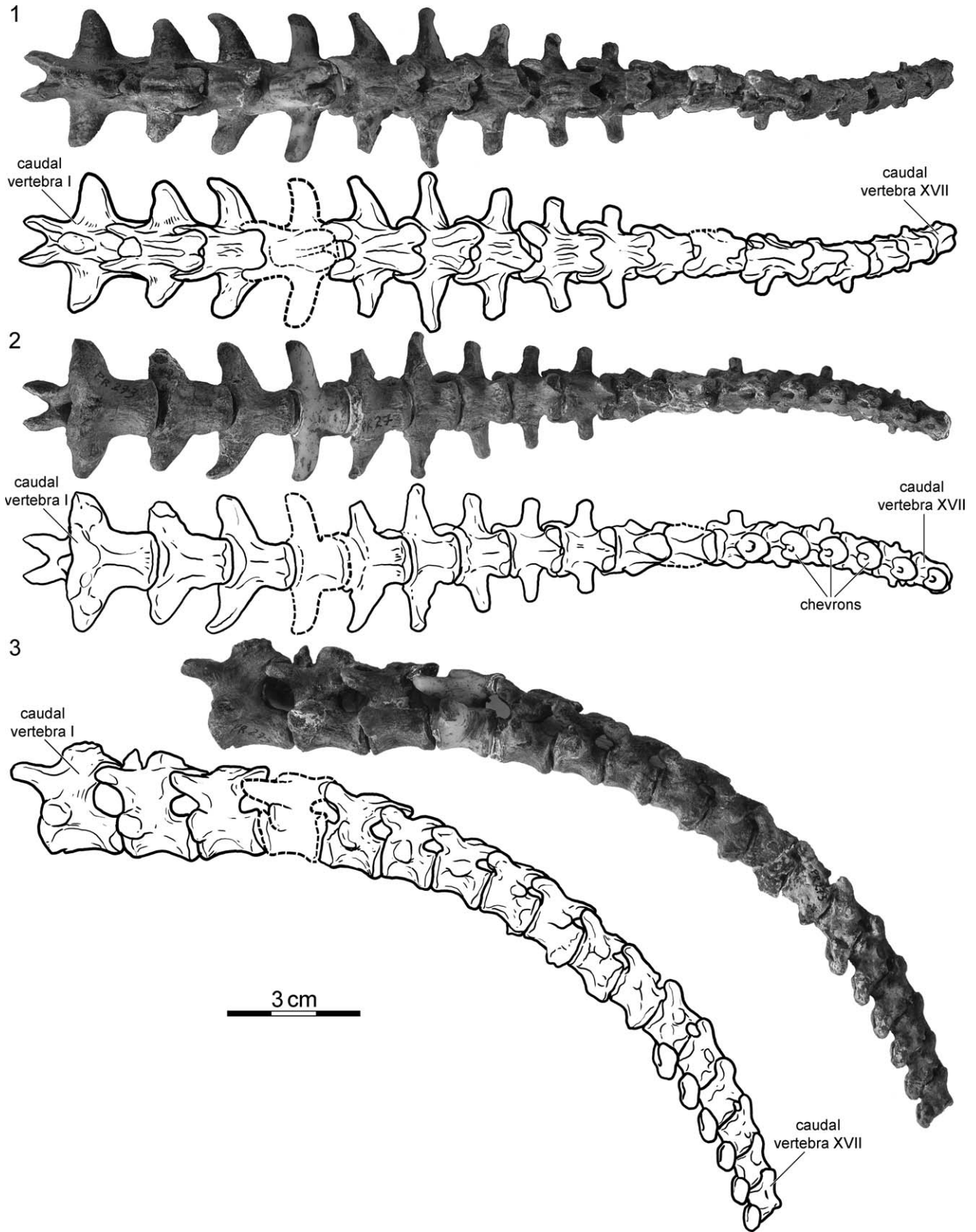


FIGURE 11—FMNH PR273, *Naomichelys speciosa*, from the Early Cretaceous (Aptian/Albian) Trinity Group of Texas, U.S.A. Photographs and illustrations of tail: 1, dorsal view; 2, ventral view; 3, left lateral view.

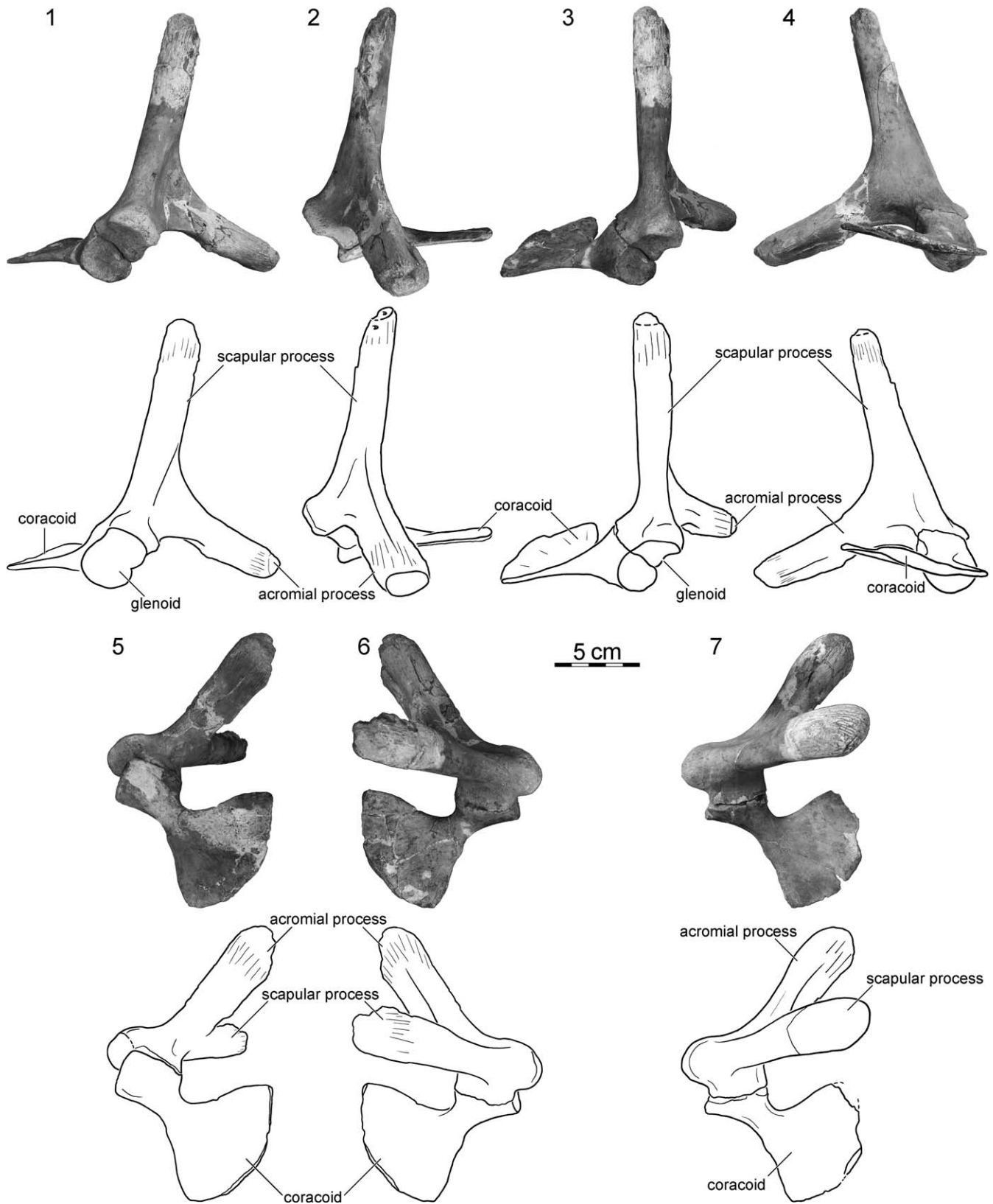


FIGURE 12—FMNH PR273, *Naomichelys speciosa*, from the Early Cretaceous (Aptian/Albian) Trinity Group of Texas, U.S.A. Photographs and illustrations of right scapulacoracoid: 1, anterolateral view; 2, anterior view; 3, posterolateral view; 4, medial view; 5, ventral view; 6, dorsal; 7, photograph and illustration of left scapulacoracoid in dorsal view.

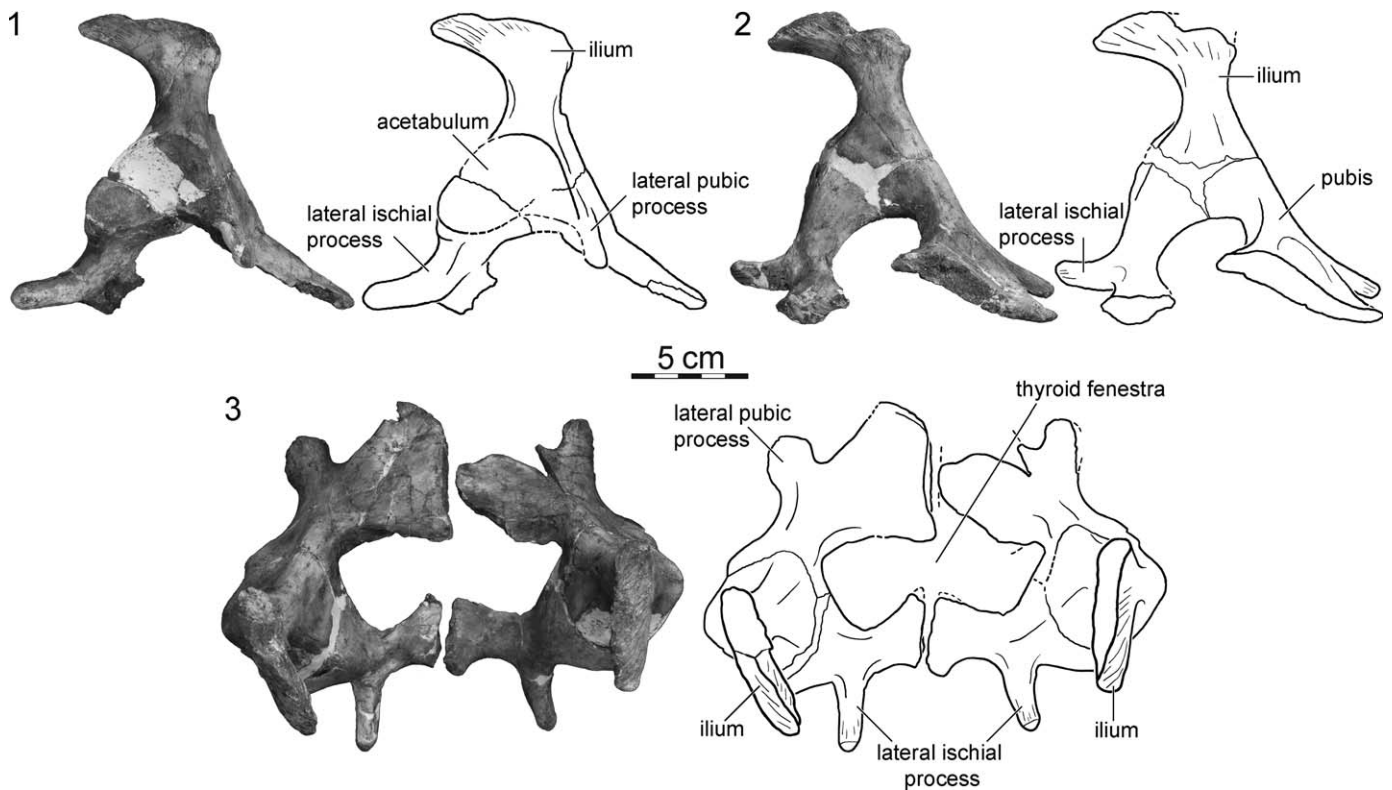


FIGURE 13—FMNH PR273, *Naomichelys speciosa*, from the Early Cretaceous (Aptian/Albian) Trinity Group of Texas, U.S.A. 1, photograph and illustration of right pelvic element in lateral view; 2, photograph and illustration of left pelvic element in medial view; 3, photograph and illustration of complete full pelvis in dorsal view.

*qiguensis*, and longer than those lateral processes present in *Pat. gasparinae*. The pubes and ischia suturally contact one another along the midline. These bones do not appear to be heavily damaged at this contact and it thereby appears that they form a large, confluent thyroid fenestra. There is no evidence for an ossified or calcified epipubis.

**Humerus.**—The right and left humeri are well preserved, but both are missing significant portions of the lateral process (Fig. 14). The proximal end of the humerus is about 50 percent more expanded than the distal end of the bone. In dorsal view, the distal expansion appears to be greatly asymmetrical, as in many turtles, by tilting towards the anterior. The humerus is more slender than in *Pr. quenstedti*, *K. bajazidi*, and *Me. platyceps*, but more robust than in crown-group turtles. Although this asymmetry is exaggerated by the absence of the missing lateral process, the shoulder of the head is clearly positioned below (or lateral) to the medial process. The head of the humerus is well defined and nearly hemispherical. A distinct shoulder is developed towards the lateral process. The medial process sits above (or medially) to the humeral head, exhibits a bulbous attachment site for muscles, and is connected to the humeral head by a stout bridge. The lateral processes are damaged on both sides. In ventral view, a broad intertubercular fossa is apparent. Within this intertubercular fossa, a deep, secondary fossa is positioned below (or lateral) to the sulcus formed by the medial process and the humeral head. The shaft of the humerus is slightly sinuous when viewed from anterior or posterior. The distal expansion of the humerus is asymmetrical and appears to mirror the proximal end by tilting anteriorly. The anterior and posterior expansions therefore form a parallelogram in dorsal or ventral view. A distinct articular surface is formed on the lateroventral side of the proximal end that is defined by a low ectepicondyle and entepicondyle. The ectepicondylar canal is enclosed and two ectepicondylar foramina

are therefore positioned along the distal end of this bone. An enclosed ectepicondylar canal is present in basal turtles such as *Pr. quenstedti*, *Pal. talampayensis*, *C. antiqua*, *Mo. efremovi*, and *Me. platyceps*.

**Radius and ulna.**—The left radius and ulna are completely preserved, but only the proximal end of both bones and the distal end of the ulna are preserved on the right side. We therefore figure only the elements from the left side (Fig. 15.1–15.4). The radius and ulna contact one another along their long axis proximally and distally and form a rounded surface proximally for articulation with the humerus and a V-shaped distal surface for articulation with the manus.

The ulna is a rather massive bone that is about 25 percent longer than the radius. The proximal and distal ends are only slightly wider than the shaft and about equal in width. As in most terrestrial turtles, the olecranon process is well developed. A distinct ridge is apparent midway along the shaft that faces the radius and that likely served as the attachment site for the bicapital tendon. The ulna exhibits two clear facets on its distal end. The lateral of these two facets articulated with the ulnare, the medial one with the intermedium.

The radius is shorter and more slender than the ulna (Fig. 15.1–15.4). The proximal end is only slightly expanded relative to the shaft, whereas the distal end is about twice as wide. A number of clearly defined ridges are present on both sides of the shaft, which served as muscle attachment sites. The radius exhibits two distinct facets distally, the medial of which articulated with the intermedium, the lateral of which with the medial centrale and perhaps also the first distal carpal.

**Manus.**—Only parts of the left manus are preserved in articulation (Fig. 15.5). Isolated phalanges and potential carpal bones are preserved in isolation with the specimen, but none could be identified with any confidence. The partial manus

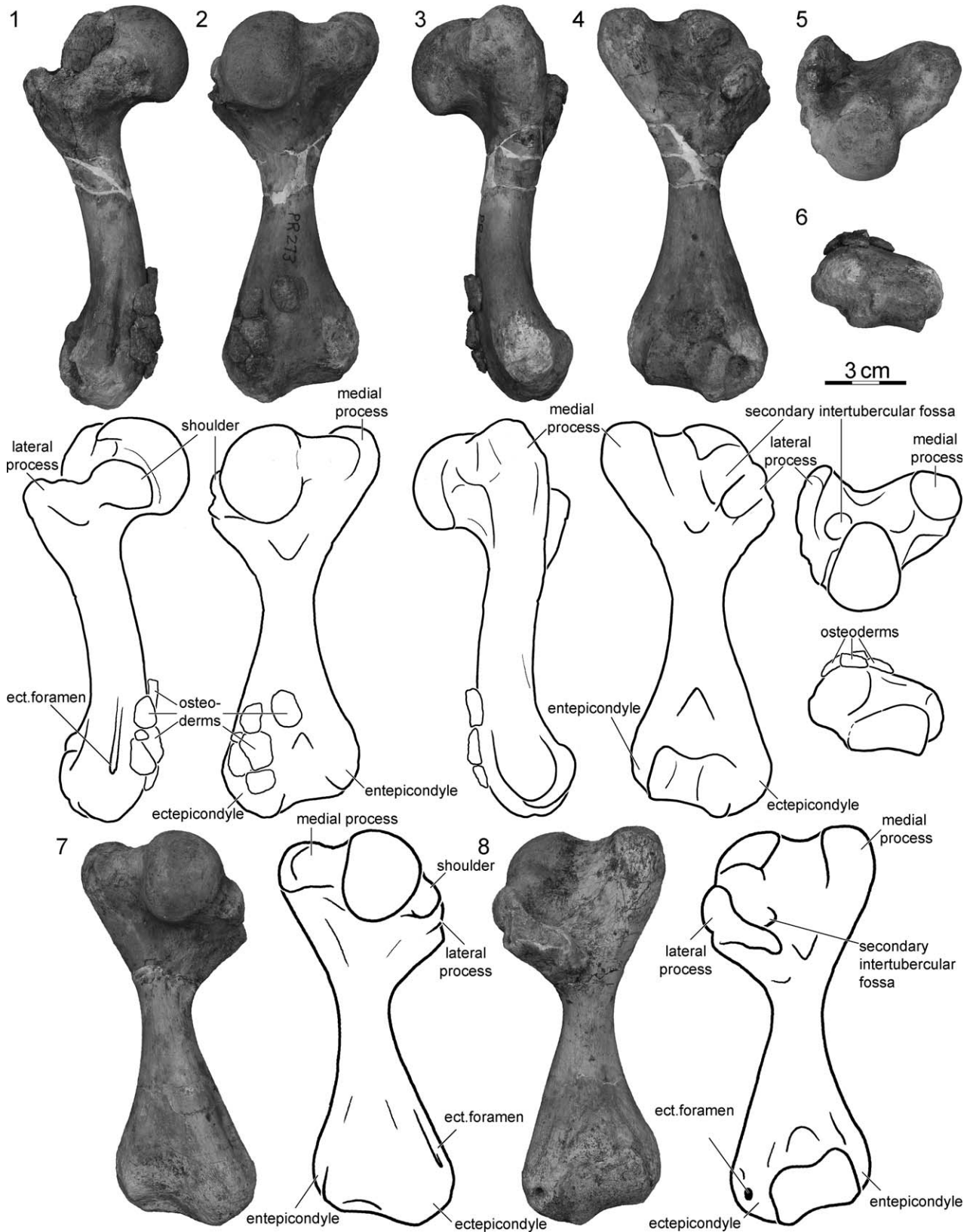


FIGURE 14—FMNH PR273, *Naomichelys speciosa*, from the Early Cretaceous (Aptian/Albian) Trinity Group of Texas, U.S.A. Photographs and illustrations of left humerus: 1, anterior view; 2, dorsal view; 3, posterior view; 4, ventral view; 5, proximal view; 6, distal view; photographs and illustrations of right humerus: 7, dorsal view; 8, ventral view. Abbreviation: ect. foramen=ectepicondylar foramen.

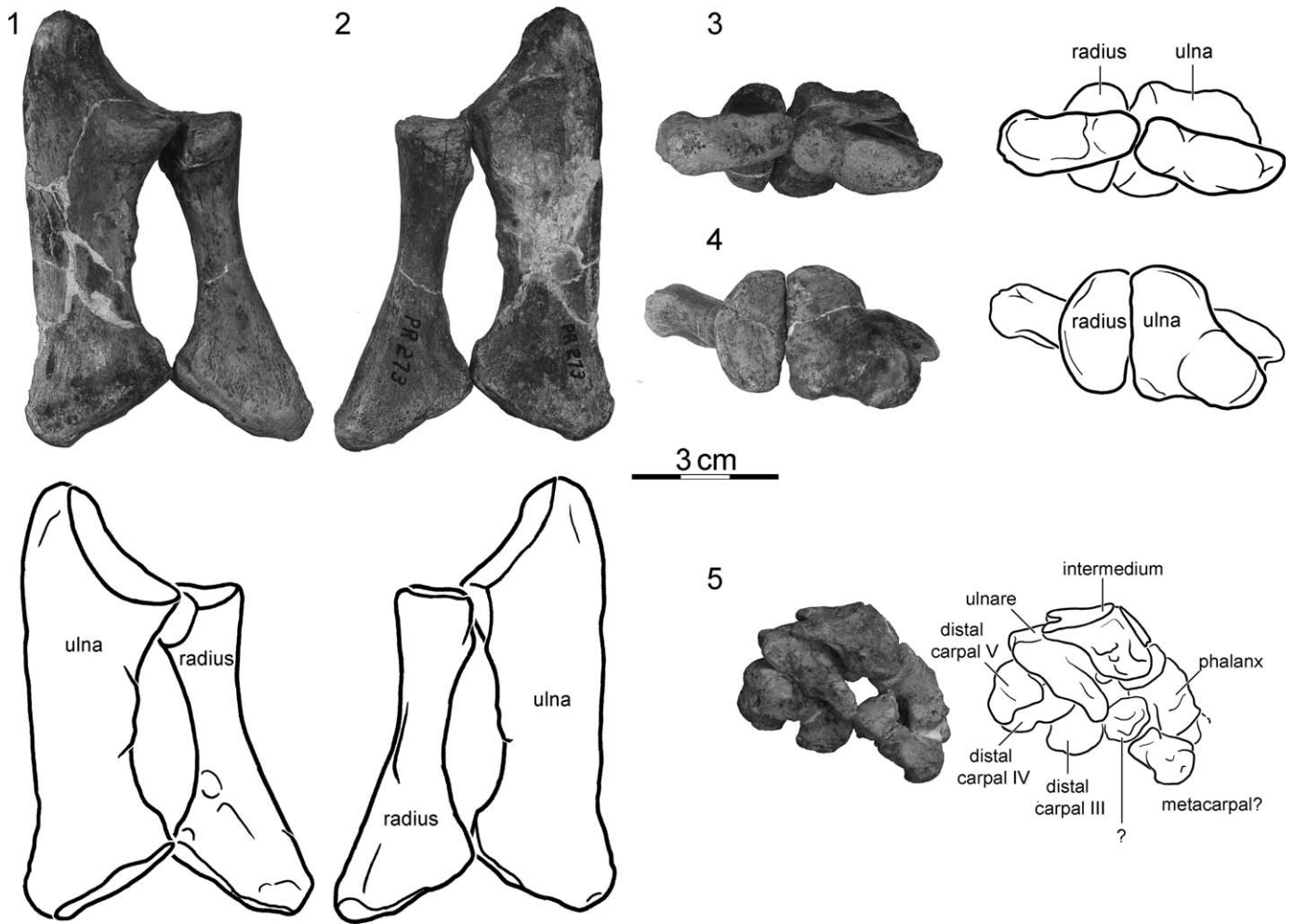


FIGURE 15—FMNH PR273, *Naomichelys speciosa*, from the Early Cretaceous (Aptian/Albian) Trinity Group of Texas, U.S.A. Photographs and illustrations of left radius and ulna: 1, ventral view; 2, dorsal view; 3, distal view; 4, proximal ventral; 5, photograph and illustration left partial manus in palmar view.

consists of the intermedium, ulnare, distal carpals III–IV, a metacarpal, a proximal phalanx, and a bone fragment of uncertain affinities.

The intermedium is a large bone and has a trapezoidal shape in dorsal view (Fig. 15.5). The intermedium exhibits two well-defined proximal articular surfaces. The lateral articular surface for the ulna is V-shaped in proximal view and the tips of the V are slightly inflated. The intermedium tightly articulates with the ulna and these inflated ends of the articular surface fit tightly into corresponding pockets at the distal end of the ulna and likely hinder torsion within the joint. The medial articular surface for the radius is semi lunar in outline in proximal view and tightly articulates with the radius. On the dorsal side of the intermedium, a number of small tubercles are apparent that likely served as attachment points for the extensor muscles. On the ventral side, the intermedium only exhibits a central, round depression. Laterodistally, the intermedium is still articulated with the ulnare, although these bones have shifted from their live position. The mediolateral articulation with the centrale(s) is only half as large as the articulation with the radiale. As these bones are missing, it is unclear if one or two centralia were present, although the shape of the radiale suggests the former presence of two (see below).

The ulnare is approximately as large as the intermedium (Fig. 15.5). It articulates proximally with the intermedium along a

slightly convex surface. Medially, the ulnare forms a dorsal and ventral process of unknown function. Laterally, the ulnare exhibits a well-developed surface for articulation with the ulna, but the two bones do not form a good fit against each other, perhaps indicating that much flexion and extension of the wrist occurred along this surface. Distally, the ulnare exhibits two articular surfaces, the lateral of which still articulates with distal carpals I and II. The second, medial surface is oriented more obliquely, away from the level of the distal carpals, and therefore suggests a void within the manus best filled by a lateral centrale.

Distal carpals II–IV are roughly cubic elements, but show some prolongation in proximodistal direction (Fig. 15.5). All distal carpals show rounded joints proximally and ball-shaped joints distally, indicating a great range of motion within this portion of the hand. The only preserved metacarpal element is as long as the distal carpals where the only preserved manual phalanx shows well-developed articular surfaces and is approximately 50 percent longer than the only preserved metatarsal. Combined, the short metacarpal and phalanx indicate a relatively short hand typical of the terrestrial to intermediate range of Joyce and Gauthier (2004). This type of hand is also found in the extinct *Pr. quenstedti*, *Pal. talampayensis*, and *Me. platyceps*.

*Femur*.—The right and left femora are both well preserved with exception of the minor trochanter, which is missing on both femora (Fig. 16). The general shape resembles that of *Pr.*

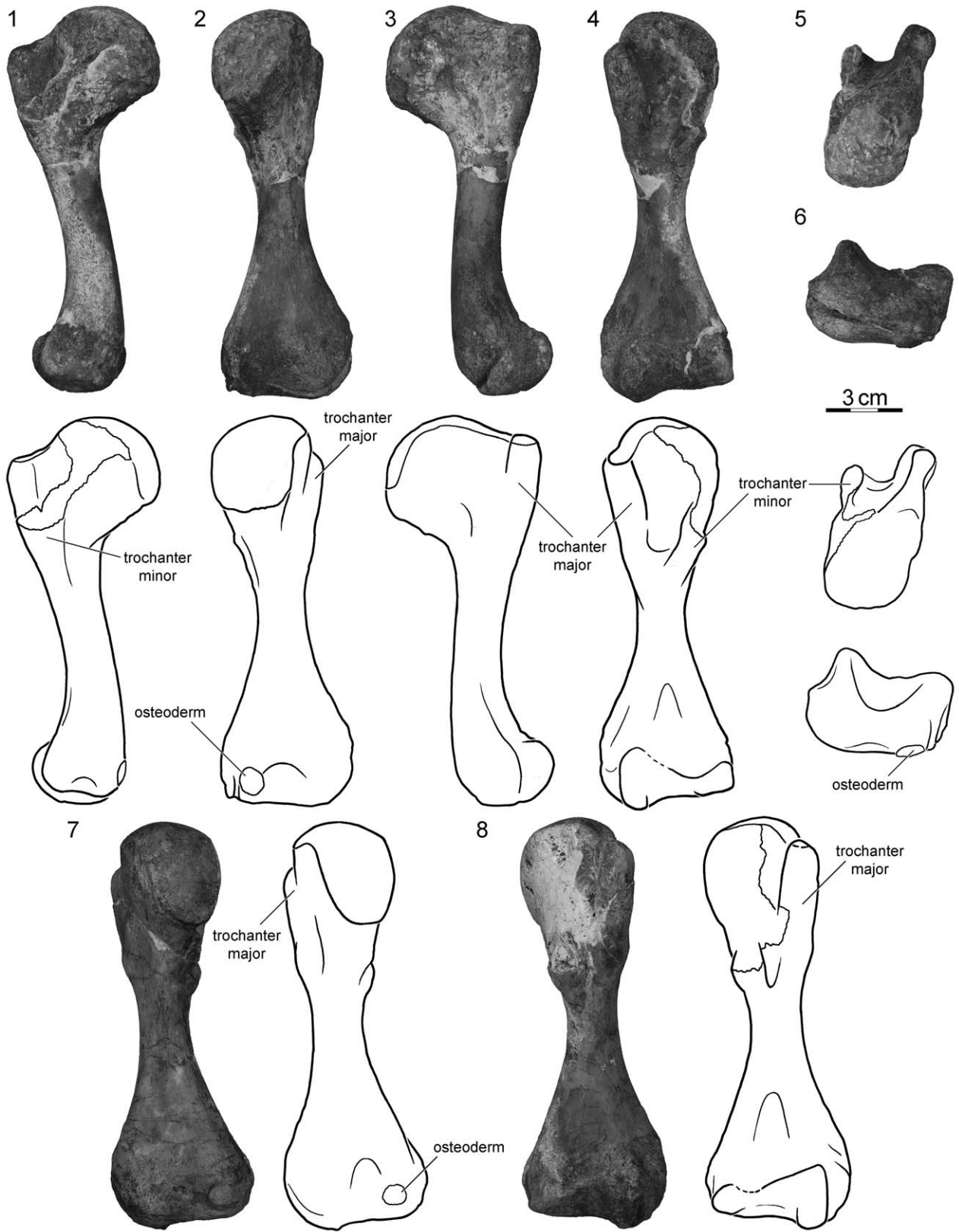


FIGURE 16—FMNH PR273, *Naomichelys speciosa*, from the Early Cretaceous (Aptian/Albian) Trinity Group of Texas, U.S.A. Photographs and illustrations of left femur: 1, anterior view; 2, dorsal view; 3, posterior view; 4, ventral view; 5, proximal view; 6, distal view; photographs and illustrations of right femur: 7, dorsal view; 8, ventral view.



*quenstedti* and *Pal. talampayensis* in that the long axis has no significant expansion at the proximal end. The femoral head is rounded, oval, and is oriented slightly oblique towards the greater trochanter and grades into the lesser trochanter. In some living, terrestrial turtles, the femoral head will also grade into the lesser trochanter, but damage in this region is too extensive to allow assessing this morphology. A deep intertrochanteric fossa is developed in ventral view. The shaft is round in cross section and only slightly sinuous in anterior or posterior view. The distal expansion of the femur is significantly greater than the proximal expansion, but this is possibly an artifact created by damage to the minor trochanter. A broad, saddle-shaped articular surface is developed on the ventrodistal end of the femur that is defined by two condyles, the posterior of which is better developed.

*Tibia and fibula.*—The tibiae and fibulae of the right and left hind limbs are preserved fully intact and can be studied from all views (Figs. 17–19). The tibia is a robust element. The proximal end is about twice as wide mediolaterally than the narrowest portion of the shaft and about three times deeper anteroposteriorly. In proximal view, two concavities are apparent on the medial side of the tibia that are separated from one another by a low ridge and that served as the articular sites for the two distal condyles of the femur (Figs. 18, 19). The patellar ridge is a well-developed, rounded anterior ridge, but no osseous patella is preserved. The top half of the straight shaft forms a rounded triangle in cross section but rapidly becomes oval distally. A distinct, slightly sinuous ridge that faces the fibula is developed along the distal half of the tibia and likely served as a muscle attachment site. Distally the tibia exhibits an anterolateral and a posteromedial condyle that closely fit into the medial articular surfaces of the astragalus.

The fibula is a straight and slender bone that is slightly longer than the tibia (Figs. 17–19). The proximal end is only slightly expanded and ends in a poorly defined articular condyle. The shaft is oval in cross section and exhibits an elongated, anteriorly facing scar just above the midline. A second muscular scar is apparent distally facing the tibia. Distally the fibula expands slightly and becomes more triangular in cross section. A single, distal condyle is developed for articulation with the lateral facet of the astragalocalcaneum. Although the two articular facets of the astragalocalcaneum contact one another, there is no evidence of an osseous contact between the tibia and the fibula.

*Pes.*—The right and left pedes are both preserved complete and in full articulation (Figs. 18, 19). The pedes were both molded and casts were produced of the dorsal view of the left foot and the palmar view of the right foot. The pedes were housed over the last decades in the molds and we decided not to remove them from their tight latex jackets as all relevant information could be gleaned from the casts and because we did not wish to jeopardize the specimen. The entire left tarsus can be removed from the left mold in articulation with the left tibia and fibula and the entire right tarsus can be removed as well. All aspects of the anatomy of this region can therefore be studied in full detail. The pes consists of the astragalocalcaneum, distal tarsals I–IV, five metatarsals, including the hooked element, and a digital formula of 2-2-3-3-3. All five unguals are recurved and claw bearing.

The astragalocalcaneum is the dominating element in the pes (Figs. 18, 19). The astragalus and calcaneum are tightly fused with one another and only hints of a suture can be found in anterior and posterior view. It is nevertheless apparent that the calcaneum is much smaller than the astragalus, being about the size of distal tarsal IV or metatarsal V. In dorsal view, the astragalocalcaneum possesses two extensive articulation sites that contact one another along a distinct ridge. The fibular articulation site is broadly concave and formed by both the astragalus and calcaneum. The tibial articulation site, by contrast, is only formed by the astragalus and is characterized by a low anteroposterior

ridge that subdivides it into two connected facets. Just ventroanteriorly to the ridge formed by the fibular and tibial articulation sites, a bulbous protrusion is apparent that forms a deep sulcus with the rim of the tibial articulation site. This sulcus is especially well developed on the right pes. The medial and posterior aspects of the astragalocalcaneum are dominated by a convex swelling that underlies significant portions of the tibial articulation site. A bulbous protrusion is also apparent below the calcaneum that may serve as a muscle attachment site associated with digit IV and/or V. The medial aspect of the calcaneum is characterized by a broad sulcus that is formed by the posterior edge of the distal tarsal IV articulation site and a well-developed crest of uncertain purpose that is situated along the posterolateral aspect of the calcaneum. The anterior and palmar aspects of the astragalocalcaneum are either covered or badly preserved and the articulation sites with distal tarsals I–III are not fully clear. It appears, however, that distal tarsal I articulates along a broad anteromedial shoulder, whereas distal tarsals II and III are located within an anterior convexity. The articulation site with distal tarsal IV is a deep and broad convexity situated along the anterolateral side of the astragalocalcaneum.

Distal tarsal I is a button shaped element that is concave proximally and convex distally (Figs. 18, 19). Distal tarsals II and III are more elongate than distal tarsal I and therefore have stout shafts that separate the convex proximal and distal articulation sites. Blunt basituberal processes are developed along the distopalmar side of these elements. A proximal articulation surface furthermore exists between distal tarsals III and IV. Distal tarsal IV is a large blocky element that is about the size of hooked metatarsal V. It articulates along a broad convexity with the astragalocalcaneum, has a blunt medial contact with distal tarsal III and a convex lateral contact with hooked metatarsal V. Distally there is a broad, convex articulation site for metatarsal IV and a distinct basituberal process for a muscle attachment site.

As in all turtles, the five metatarsals, including the ansulate (Joyce et al., 2013), articulate with one another in an inward, shingling manner (Figs. 18, 19). Metatarsal I is as short as the ansulate and has a greatly expanded base. Although metatarsals II and III increase in length, the distal articular surfaces of metatarsals I–III align with one another. Metatarsal IV and the ansulate decrease in size and their distal ends therefore do not line up with the first three metatarsal elements. Various scars are apparent along the shaft of these elements for the interdigital musculature. The ansulate is the shortest, but proximally widest metatarsal element. Its medial border exhibits a broad muscle scar that grades into the convex articulation site for the first phalanx of digit V.

The phalangeal formula is 2-2-3-3-3 on both feet (Figs. 18, 19). All unguis elements are slightly recurved and clearly show signs of having possessed a claw. The first phalanx of the fifth digit is notable for only being half as long as metatarsal IV. The combined length of the phalanges of digit III is about as long as metatarsal III.

*Osteoderms.*—The great level of completeness of FMNH PR273 is further underlined by the large number (ca. 250) of osteoderms that were found accompanying the skeleton (Figs. 17–20). The majority of osteoderms were collected in vials during preparation and it is therefore at first unclear from which part of the skeleton they originate. However, a paper tag indicates that a collection of approximately 30 small osteoderms originated from the neck region, and numerous larger osteoderms remain in articulation with the limbs (Figs. 17–19). Many of the large limb osteoderms have unique sizes and shapes, and it is therefore possible to identify their right or left counterparts among the isolated element. It is therefore apparent that small osteoderms

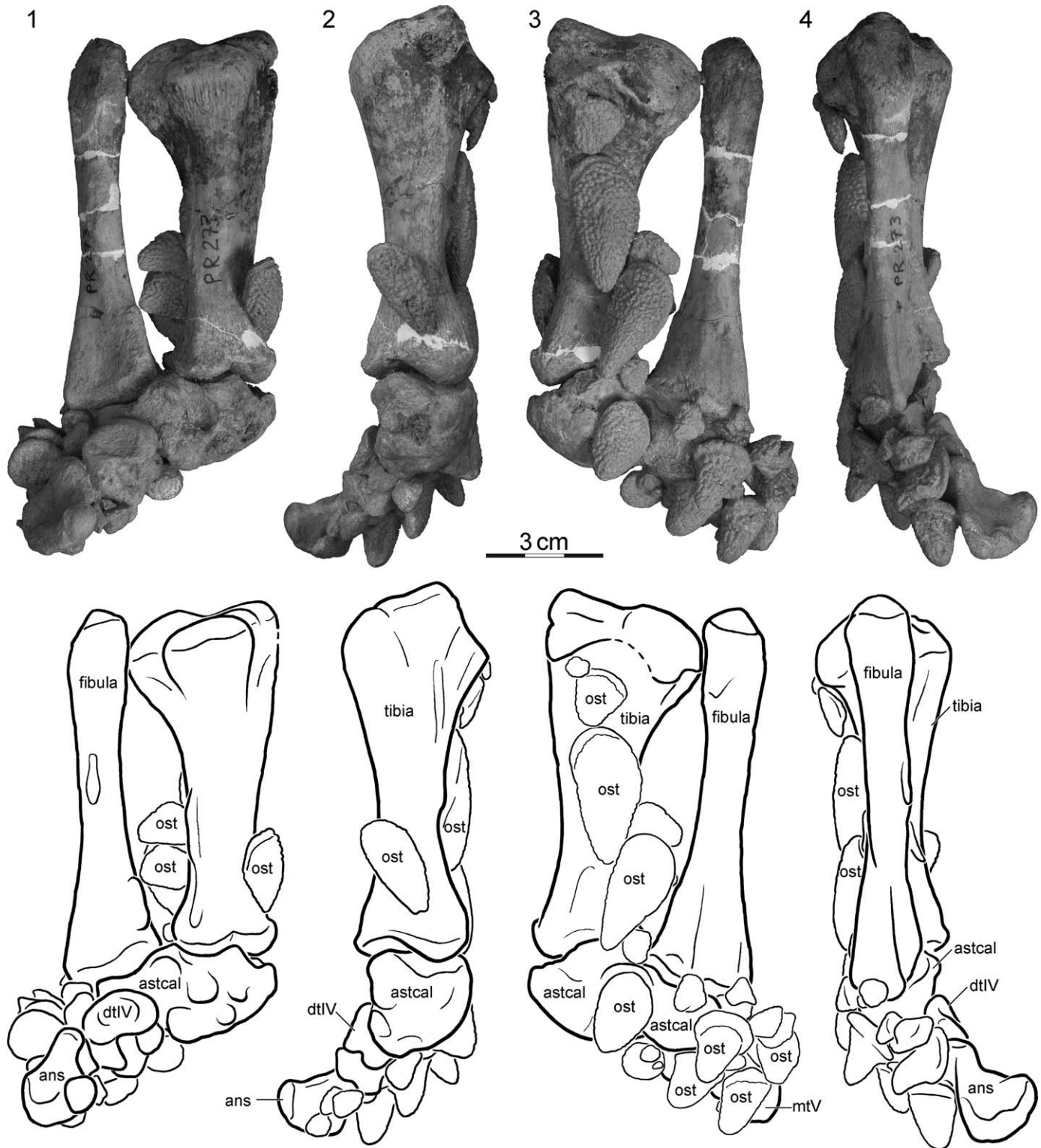


FIGURE 17—FMNH PR273, *Naomichelys speciosa*, from the Early Cretaceous (Aptian/Albian) Trinity Group of Texas, U.S.A. Photographs and illustrations of right tibia, fibula, and partial pes: 1, dorsal view; 2, medial view; 3, ventral view; 4, lateral view. Abbreviations: ans=ansulate; astcal=astagalus-calcaneum; dt=distal tarsal; mt=metatarsal; ost=osteoderm.

covered the neck, medium to large sized osteoderms covered the lower arms and wrists, and that medium-sized osteoderms covered the ankles.

The limb osteoderms are cone shaped, but the apices are typically displaced relative to the base of the element (Fig. 20.1—

20.4). In the articulated specimens, all apices are directed distally (Figs. 17, 18). The largest elements are associated with the posterior side of the arms (Fig. 20.1), medium sized element adorn the wrists and ankles. The visceral concavity is deeper than in the neck osteoderms. The base is often separated by a ring from

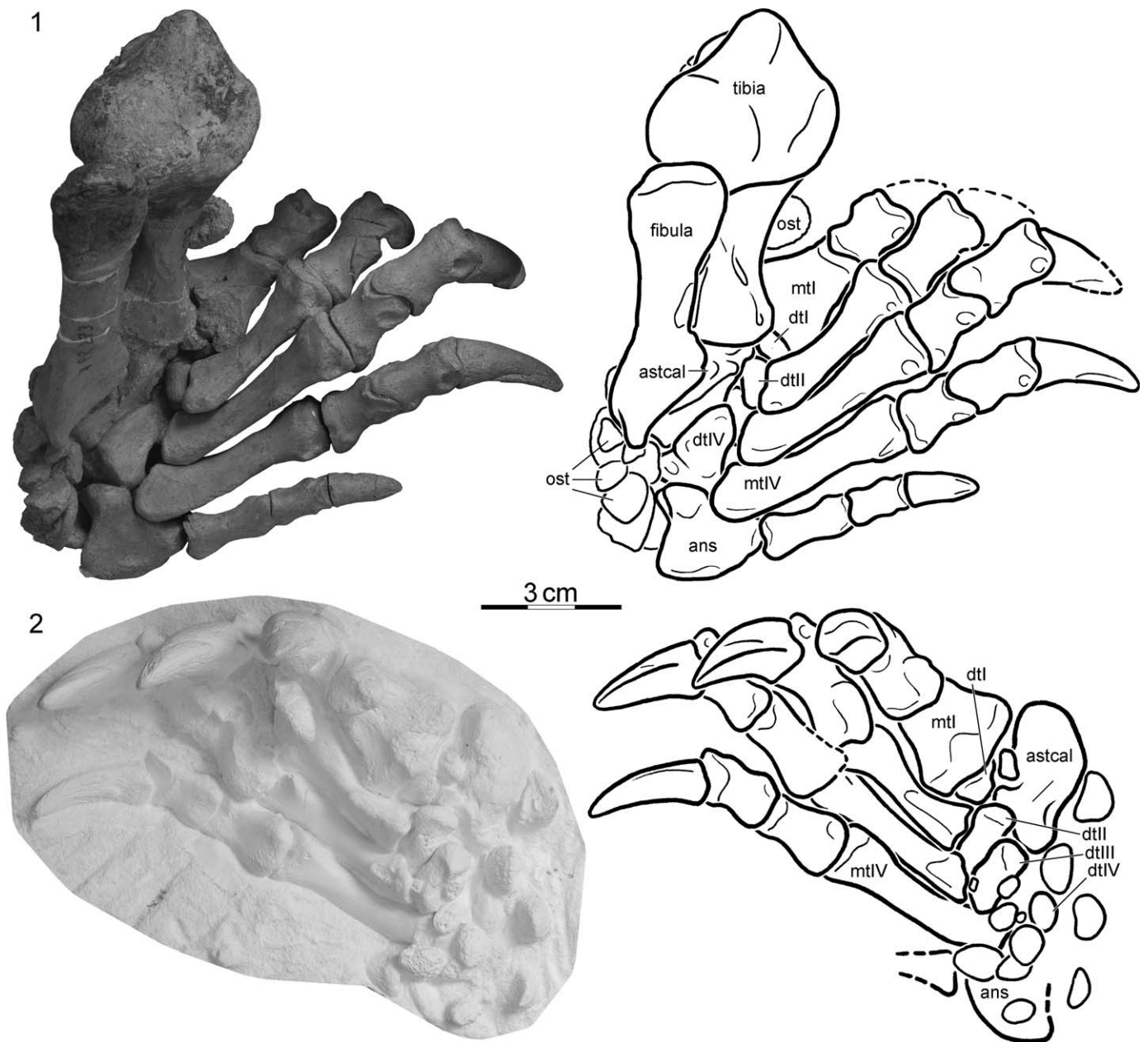


FIGURE 18—FMNH PR273, *Naomichelys speciosa*, from the Early Cretaceous (Aptian/Albian) Trinity Group of Texas, U.S.A. Photographs and illustrations of right tibia, fibula, and pes: 1, dorsal view; 2, ventral/palmar view. Abbreviations: ans=ansulate; astcal=astragalus-calcaneum; dt=distal tarsal; mt=metatarsal; ost=osteoderm.

the remaining part of the element, which probably helped anchor the element in the skin. The 30 known neck osteoderms are small, round elements with a concentrically placed modest apex and a slight visceral concavity (Fig. 20.5). All osteoderms show the same surface sculpturing as the shell and cranium. Limb osteoderms have otherwise been reported for *Pr. quenstedti*, *S. vermiculata* and *Me. platyceps*. Isolated osteoderms (“granicones”) from the Early Cretaceous of England have referred to *Solemydidae* by explicit reference to FMNH PR273 (Barrett et al., 2002).

#### DISCUSSION

*Taxonomic considerations.*—With exception of the beautifully preserved skeleton described herein (FMNH PR273), the entire published fossil record of North American solemydid turtles is

restricted to Aptian to Campanian fragments found throughout the continent (Joyce et al., 2011). The holotype of *Naomichelys speciosa* consists of an isolated entoplastron that was found in Aptian sediments near the town of Pryor, Montana (AMNH 6136; Hay, 1908, pl. 40, figs. 2, 3). As Joyce et al. (2011) already noted, the surface sculpturing preserved in the type specimen of *N. speciosa* is highly diagnostic for Solemydidae, but does not differ significantly from the sculpturing seen in a number of European solemydids, in particularly the Aptian/Albian *Helochelydra nopcsai* and the Cenomanian *Helochelys danubina* von Meyer, 1855. *Naomichelys speciosa* is therefore diagnosed in part by originating from North America and all North American material was traditionally referred to this taxon for a lack of better alternatives.

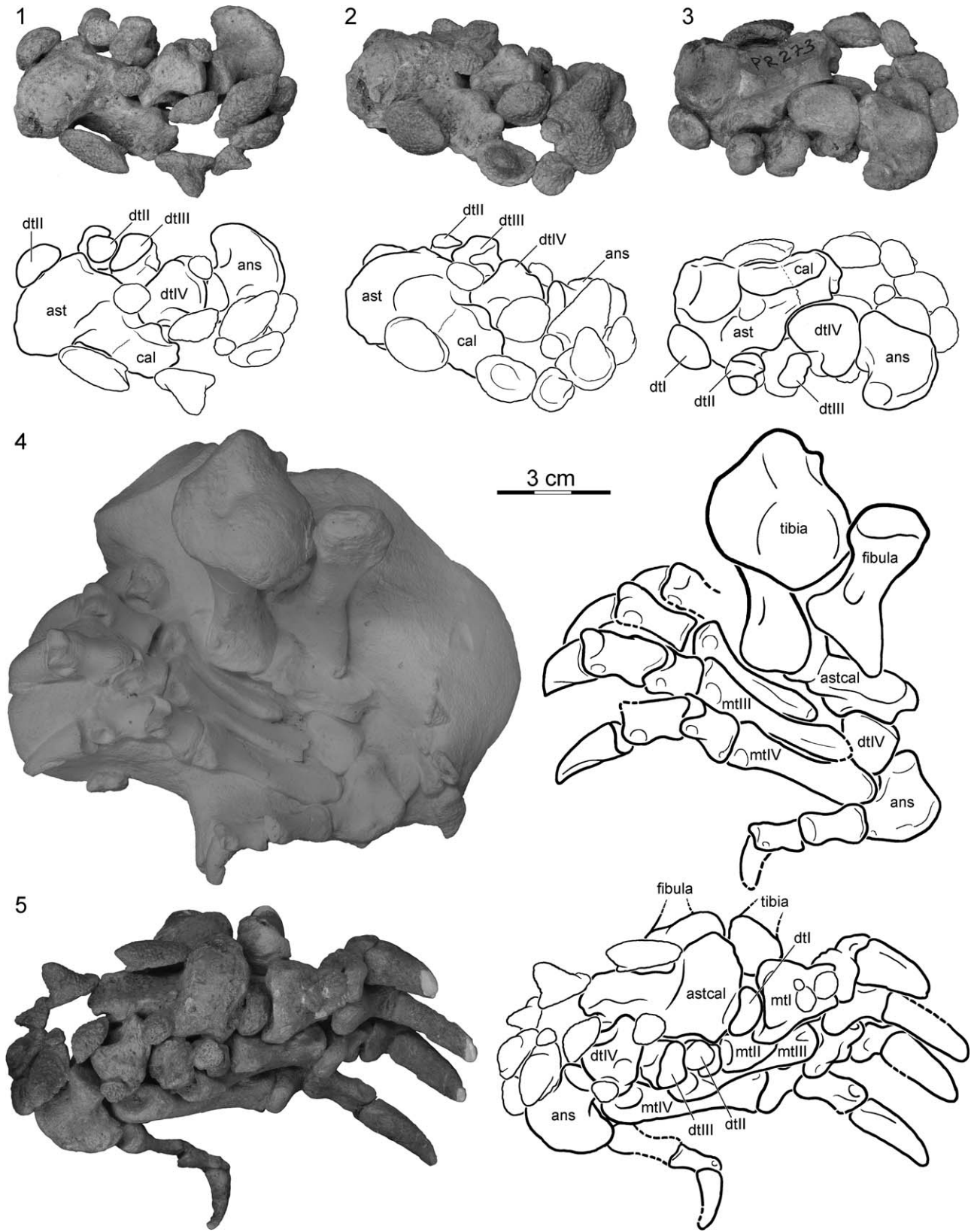


FIGURE 19—FMNH PR273, *Naomichelys speciosa*, from the Early Cretaceous (Aptian/Albian) Trinity Group of Texas, U.S.A. 1–3, photographs and illustrations of left partial pes in three oblique views; left tibia, fibula, and pes: 4, dorsal view; 5, ventral/palmar view. Abbreviations: ans=ansulate; ast=astragalus; astcal=astragalus-calcaneum; cal=calcaneum; dt=distal tarsal; mt=metatarsal. All non-labeled elements associated with the metatarsus are osteoderms.

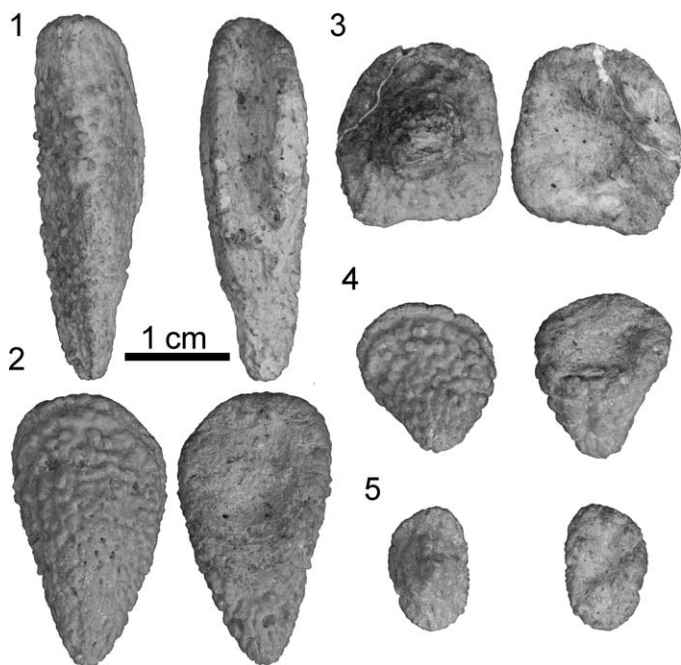


FIGURE 20—FMNH PR273, *Naomichelys speciosa*, from the Early Cretaceous (Aptian/Albian) Trinity Group of Texas, U.S.A. 1–5, photographs of five different osteoderms from external (left) and visceral (right) view.

Given the fragmentary nature of the solemydid fossil record, FMNH PR273 provides an unprecedented level of anatomical information. Ironically, the anterior plastron elements, including the entoplastron, are among the poorest preserved portions of the shell and comparison with the holotype of *N. speciosa* is therefore limited. The visceral aspects and the outline of the entoplastron of FMNH PR273 are poorly preserved and we therefore refrain from making comparisons with the holotype. The entoplastron of FMNH PR273 and the holotype of *N. speciosa* otherwise resemble one another by having similarly sized and shaped entoplastral scutes, tubercles that do not coalesce, and a gular/humeral sulcus that is curved towards the anterior. However, the sculpturing of FMNH PR273 is finer than that of the holotype (i.e., tubercles are smaller and more densely arranged) and the tubercles are not arranged in rows that run parallel to the sulcus of the entoplastron, as seen in the holotype. FMNH PR273 and the holotype of *N. speciosa* were both recovered from Aptian/Albian sediments from the same continent (Fig. 1) and, yet, the Aptian/Albian spans 25 million years and the localities are separated by approximately 1500 km from one another. We nevertheless follow previous authors (Hirayama et al., 2000; Barrett et al., 2002; Scheyer and Anquetin, 2008; Anquetin, 2012) by referring FMNH PR273 to *N. speciosa*. The minute differences in the morphology of the entoplastron are therefore interpreted as interspecies variation and *N. speciosa* is interpreted as having a great temporal and spatial distribution. A shell recently announced from the Campanian of British Columbia (Larson et al., 2010) should provide enough information to test this taxonomic arrangement, but it may also reveal *N. speciosa* to be a nomen dubium.

The vast majority of solemydid taxa were named during the 19<sup>th</sup> century based on highly fragmentary material. Joyce et al. (2011) noted that most of these taxa lack clear autapomorphies, but given that they originate from distinct geographic areas and/or time intervals, Joyce et al. (2011) cautiously recognized their validity and speculated that additional material will likely support

this assessment. The shell sculpturing of *H. nopcsai* from the Aptian/Albian of England, *H. danubina* from the Cenomanian of Germany, *N. speciosa* from the Aptian/Albian of North America, and fragmentary specimens from the Lower Cretaceous of Spain (Pérez-García et al., 2013) greatly resemble one another and it therefore has previously not been possible to rigorously diagnose these taxa. Though incomplete, the skull of FMNH PR273 allows for the first time to make a direct comparison with that of *H. nopcsai*, the only other solemydid skull currently known. In overall gestalt, both skulls resemble one another greatly by lacking temporal emarginations, by having laterally set orbits, and an anteriorly sloping snout. The skull of both taxa are typical for derived stem turtles by having relatively small prefrontals that do not meet one another along the midline, elongate postorbital, jugals that do not contribute to the orbit, and the absence of supratemporals. *Naomichelys speciosa* and *H. nopcsai* share a number of unique synapomorphies in the skull, including a posterior expansion of the squamosals, the presence of triangular fossae that are formed by the squamosals behind the cavum tympani, the formation of a second pair of tubercular basioccipitale by the pterygoids, foramina pro ramo nervi vidiani (VII) that are visible in ventral view, and an apparent lack of an osseous subdivisions between the cavum acustico-jugulare and recessus scalae tympani absent. The skull of *N. speciosa* can easily be distinguished from that of *H. nopcsai* because the parabasi-sphenoid complex is not covered by greatly expanded pterygoids. The highly unusual mandible of *N. speciosa*, in which the dentaries form an expanded symphyseal shelf and the coronoid process are flattened ventromedially, furthermore allows firmly distinguishing *N. speciosa* from *H. nopcsai*. These differences in the skull collectively confirm the validity of both taxa and reveal that a significant amount of cranial variation is apparent in the skulls of solemydid turtles.

#### ACKNOWLEDGMENTS

We wish to thank P. Makovicky, A. Shinya, W. Simpson, and O. Rieppel (FMNH) for generously providing access to the specimen described herein. The gray tone art of the skull used herein was produced by R. Laws, the images of the skull were produced by P. Crabb (NHM Photo Studio), whereas the line drawings of the cervical and caudal vertebrae were produced by J. González. I. Werneburg and H. Sherf (University of Tübingen) are thanked for producing the CT scans used in this study. We thank Y. Y. Zhen (AM), C. Mehling (AMNH), C. Schaff (MCZ), I. Percival (MM), J. Gillette (MNA), J. Müller (NMB), V. Sukhanov (PIN), R. Schoch (SMNS), T. Rowe (TMM), P. Holroyd (UCMP), and D. Brinkman (YPM) for providing access to comparative material. Two anonymous reviewers are acknowledged for carefully reading an earlier draft of this manuscript and for providing constructive criticisms. This study was funded by a grant by the University of Tübingen to WGJ.

#### REFERENCES

- ANQUETIN, J. 2010. The anatomy of the basal turtle *Eileanchelys waldmani* from the Middle Jurassic of the Isle of Skye, Scotland. *Earth and Environmental Science Transactions of the Royal Society of Edinburgh*, 101:67–96.
- ANQUETIN, J. 2012. Reassessment of the phylogenetic interrelationships of basal turtles (Testudinata). *Journal of Systematic Palaeontology*, 10:3–45.
- ANQUETIN, J., P. M. BARRETT, M. E. H. JONES, S. MOORE-FAY, AND S. E. EVANS. 2009. A new stem turtle from the Middle Jurassic of Scotland: New insights into the evolution and palaeoecology of basal turtles. *Proceedings of the Royal Society B: Biological Sciences*, 276:879–886.
- BARRETT, P. M., J. B. CLARKE, D. B. BRINKMAN, S. D. CHAPMAN, AND P. C. ENSON. 2002. Morphology, histology and identification of the ‘granicones’ from the Purbeck Limestone Formation (Lower Cretaceous: Berriasian) of Dorset, southern England. *Cretaceous Research*, 23:279–295.

- BAUR, G. 1887. Osteologische Notizen über Reptilien (Fortsetzung II). *Zoologischer Anzeiger*, 10:241–268.
- CIFELLI, R. L., J. D. GARDNER, R. L. NYDAM, AND D. L. BRINKMAN. 1997. Additions to the vertebrate fauna of the Antlers Formation (Lower Cretaceous), southeastern Oklahoma. *Oklahoma Geology Notes*, 57:124–131.
- COPE, E. D. 1877. On reptilian remains from the Dakota Beds of Colorado. *Proceedings of the American Philosophical Society*, 17:193–196.
- EVANS, J. AND T. S. KEMP. 1975. The cranial morphology of a new Lower Cretaceous turtle from southern England. *Palaeontology*, 18:25–40.
- EVANS, J. AND T. S. KEMP. 1976. A new turtle skull from the Purbeckian of England and a note on the early dichotomies of cryptodire turtles. *Palaeontology*, 19:317–324.
- GAFFNEY, E. S. 1972. The systematics of the North American family Baenidae (Reptilia, Cryptodira). *Bulletin of the American Museum of Natural History*, 147:243–319.
- GAFFNEY, E. S. 1979. The Jurassic turtles of North America. *Bulletin of the American Museum of Natural History*, 162:91–135.
- GAFFNEY, E. S. 1983. The cranial morphology of the extinct horned turtle, *Meiolania platyceps*, from the Pleistocene of Lord Howe Island, Australia. *Bulletin of the American Museum of Natural History*, 175:361–480.
- GAFFNEY, E. S. 1985. The cervical and caudal vertebrae of the cryptodiran turtle, *Meiolania platyceps*, from the Pleistocene of Lord Howe Island, Australia. *American Museum Novitates* 2805:1–29.
- GAFFNEY, E. S. 1990. The comparative osteology of the Triassic turtle *Proganochelys*. *Bulletin of the American Museum of Natural History*, 194:1–263.
- GAFFNEY, E. S. 1996. The postcranial morphology of *Meiolania platyceps* and a review of the Meiolaniidae. *Bulletin of the American Museum of Natural History*, 229:1–166.
- GAFFNEY, E. S. AND P. A. MEYLAN. 1992. The Transylvanian turtle, *Kallokibotion*, a primitive cryptodire of Cretaceous age. *American Museum Novitates*, 3040:1–37.
- GAFFNEY, E. S., J. H. HUTCHISON, F. A. JENKINS, JR., AND L. J. MEEKER. 1987. Modern turtle origins: the oldest known cryptodire. *Science*, 237:289–291.
- GAFFNEY, E. S., T. H. RICH, P. VICKERS-RICH, A. CONSTANTINE, R. VACCA, AND L. KOOL. 2007. *Chubutemys*, a new Eucryptodiran turtle from the Early Cretaceous of Argentina, and the relationships of the Meiolaniidae. *American Museum Novitates*, 3599:1–35.
- HAY, O. P. 1908. The fossil Turtles of North America. Carnegie Institution of Washington, Washington, D.C.
- HIRAYAMA, R., D. B. BRINKMAN, AND I. G. DANILOV. 2000. Distribution and biogeography of non-marine Cretaceous turtles. *Russian Journal of Herpetology*, 7:181–198.
- HUTCHISON, J. H. AND D. M. BRAMBLE. 1981. Homology of the plastral scales of the Kinosternidae and related turtles. *Herpetologica*, 37:73–85.
- JOYCE, W. G. 2007. Phylogenetic relationships of Mesozoic turtles. *Bulletin of the Peabody Museum of Natural History*, 48:3–102.
- JOYCE, W. G. AND C. J. BELL. 2004. A review of the comparative morphology of extant testudinoid turtles (Reptilia: Testudines). *Asiatic Herpetological Research*, 10:53–109.
- JOYCE, W. G. AND J. A. GAUTHIER. 2004. Palaeoecology of Triassic stem turtles sheds new light on turtle origins. *Proceedings of the Royal Society of London, B*, 271:1–5.
- JOYCE, W. G., S. D. CHAPMAN, R. T. J. MOODY, AND C. A. WALKER. 2011. The skull of the solemydid turtle *Helochelydra nopcsai* from the Early Cretaceous (Barremian) of the Isle of Wight (UK) and a review of Solemydidae. *Special Papers in Paleontology*, 86:75–97.
- JOYCE, W. G., I. WERNEBURG, AND T. R. LYSON. 2013. The hooked element in the pes of turtles (Testudines): A global approach to exploring primary and secondary homology. *Journal of Anatomy*, 223:421–441.
- KHOSATZKY, L. I. 1997. Big turtle of the late Cretaceous of Mongolia. *Russian Journal of Herpetology*, 4:148–154.
- KLEIN, I. T. 1760. *Klassifikation und kurze Geschichte der Vierfüßigen Thiere* (translation by F. D. Behn). Jonas Schmidt, Lübeck.
- LAPPARENT DE BROIN, F. DE AND X. MURELAGA. 1996. Une nouvelle faune de chéloniens dans le Crétacé supérieur européen. *Comptes Rendus de l'Académie des Sciences, Sciences de la Terre et des Planètes, Série Iia*, 323:729–735.
- LAPPARENT DE BROIN, F. DE AND X. MURELAGA. 1999. Turtles from the Upper Cretaceous of Laño (Iberian peninsula). *Estudios del Museo de Ciencias Naturales de Alava*, 14:135–211.
- LARSON, D., D. BRINKMAN, AND J. MORIN. 2010. Late Cretaceous Canadian specimens of family Solemydidae (Testudines) with special mention of a new genus and species. *Journal of Vertebrate Paleontology, Program and Abstracts* 2010, 120A.
- LYSON, T. R., B.-A. S. BHULLAR, G. S. BEVER, W. G. JOYCE, K. DE QUEIROZ, A. ABZHANOV, AND J. A. GAUTHIER. 2013. Homology of the enigmatic nuchal bone reveals novel reorganization of the shoulder girdle in the evolution of the turtle shell. *Evolution and Development*, 15:317–325.
- MATZKE, A. T., M. W. MAISCH, G. SUN, H. PFRETZSCHNER, AND H.H. STÖHR. 2004. A new xinjiangchelyid turtle (Testudines, Eucryptodira) from the Jurassic Qigu Formation of the Southern Junggar Basin, Xinjiang, North-West China. *Palaeontology*, 47:1267–1299.
- MEYER, H. VON. 1855. *Helochelys danubina* aus dem Grünsande von Kelheim in Bayern. *Palaeontographica*, 4:96–105.
- NOPCSA, F. B. 1923. *Kallokibotion*, a primitive amphichelydean tortoise from the uppermost Cretaceous of Hungary. *Palaeontologia Hungarica*, 1:1–34.
- NYDAM, R. L. AND R. L. CIFELLI. 2002. Lizards from the Lower Cretaceous (Aptian–Albian) Antlers and Cloverly formations. *Journal of Vertebrate Paleontology*, 22:286–298.
- OWEN, R. 1842. Report on British fossil reptiles, Part II. Report for the British Association for the Advancement of Science, 11:60–204.
- OWEN, R. 1886. Description of fossil remains of two species of a *Megalania* genus (*Meiolania*, Ow.), from Lord Howe's Island. *Proceedings of the Royal Society of London*, 40:315–316.
- PÉREZ-GARCÍA, A., T. M. SCHEYER, AND X. MURELAGA. 2013. The turtles from the uppermost Jurassic and Early Cretaceous of Galve (Iberian Range, Spain): Anatomical, systematic, biostratigraphic, and palaeobiogeographical implications. *Cretaceous Research*, 44:64–82.
- RABI, M., C.-F. ZHOU, O. WINGS, S. GE, AND W. G. JOYCE. 2013. A new xinjiangchelyid turtle from the Middle Jurassic of Xinjiang, China and the evolution of the basipterygoid process in Mesozoic turtles. *BMC Evolutionary Biology*, 13/203:1–20.
- REYNOSO, V.-H. 2006. Research on fossil amphibians and reptiles in Mexico, from 1869 to early 2004 (including marine forms but excluding pterosaurs, dinosaurs, and obviously, birds). *Studies on Mexican Paleontology*, 24:209–231.
- ROUGIER, G. W., M. S. DE LA FUENTE, AND A. B. ARCUCCI. 1995. Late Triassic turtles from South America. *Science*, 268:855–858.
- SCHEYER, T. M. AND J. ANQUETIN. 2008. Bone histology of the Middle Jurassic turtle shell remains from Kirtlington, Oxfordshire, England. *Lethaia*, 41:85–96.
- SMITH, E.T. AND B. P. KEAR. 2013. *Spoochelys ormondea* gen. et sp. nov., an archaic Meiolaniid-like turtle from the Early Cretaceous of Lightning Ridge, Australia, p. 121–146. *In* D. B. Brinkman, P. A. Holroyd, J. D. Gardner (eds.), *Morphology and Evolution of Turtles: Vertebrate Paleobiology and Paleoanthropology*. Springer, Dordrecht.
- STERLI, J. 2008. A new, nearly complete stem turtle from the Jurassic of South America with implications for turtle evolution. *Biology Letters*, 4:286–289.
- STERLI, J. AND M. S. DE LA FUENTE. 2010. Anatomy of *Condorchelys antiqua* Sterli 2008 and the origin of modern jaw closure mechanism in turtles. *Journal of Vertebrate Paleontology*, 30:251–366.
- STERLI, J. AND M. S. DE LA FUENTE. 2011. A new turtle from the La Colonia Formation (Campanian–Maastrichtian), Patagonia, Argentina, with remarks on the evolution of the vertebral column in turtles. *Palaeontology*, 54:63–78.
- STERLI, J., M. S. DE LA FUENTE, AND A. M. UMAYANO. In press. New remains and new insights on the Gondwanan meiolaniform turtle *Chubutemys copelloi* from the Lower Cretaceous of Patagonia, Argentina. *Gondwana Research*, <http://dx.doi.org/10.1016/j.gr.2013.08.016>.
- STERLI, J., M. S. DE LA FUENTE, AND G. W. ROUGIER. 2007. Anatomy and relationships of *Palaeochersis talampayensis*, a Late Triassic turtle from Argentina. *Palaeontographica Abteilung A*, 281:1–61.
- STERLI, J. AND JOYCE, W. G. 2007. The cranial anatomy of the Early Jurassic turtle *Kayentachelys aprix*. *Acta Paleontologica Polonica*, 52:675–694.
- STERLI, J., J. MÜLLER, J. ANQUETIN, AND A. HILGER. 2010. The parabasisphenoid complex in Mesozoic turtles and the evolution of the testudinate basicranium. *Canadian Journal of Earth Sciences*, 47:1337–1346.
- SUKHANOV, V. B. 2006. An archaic turtle, *Heckerochelys romani* gen. et sp. nov., from the Middle Jurassic of Moscow Region, Russia. *Fossil Turtle Research*, 1:112–118.

ACCEPTED 10 MARCH 2014

## APPENDIX 1

Representative measurement of FMNH PR273, *Naomichelys speciosa*, from the Early Cretaceous (Aptian/Albian) Trinity Group of Texas, U.S.A.

*Skull (as reconstructed)*

midline length (snout to occipital condyle): 110 mm  
width at mandibular condyles: 85 mm

*Shell*

midline carapace length: 72.5 cm  
carapace length, straight measurement, including peripheral shoulders: 80 cm

carapace width: 66 cm  
plastron midline length, straight measurement: 60 cm  
anterior plastral lobe at base: 34 cm  
posterior plastral lobe at base: 31 cm  
bridge at narrowest point: 27 cm

*Pectoral Girdle*

acromion process to shaft of scapular process: 110 mm  
pectoral process to rim of glenoid: 130 mm  
coracoid to rim of glenoid: 90 mm  
maximum width of coracoid: 75 mm

*Forelimb*

length of humerus between articular surfaces: 135 mm  
maximum length of humerus: 143 mm  
maximum length of ulna: 85 mm  
maximum length of radius: 66 mm

*Hind Limb*

maximum length of femur: 148 mm  
lateral length of fibula: 90 mm  
lateral length of tibia: 90 mm  
length metatarsal III: 47 mm  
approximate length of digit III, inclusive of metatarsal III: 107 mm